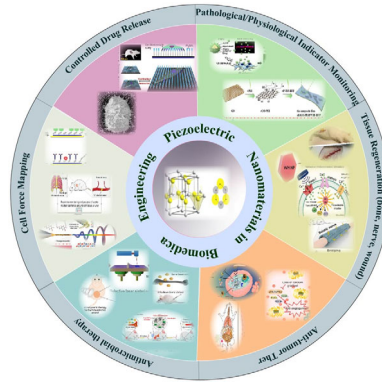


REVIEWS

J. Ji, C. Yang, Y. Shan, M. Sun, X. Cui,
L. Xu, S. Liang, T. Li, Y. Fan, D. Luo,*
Z. Li* 2200088

Research Trends of Piezoelectric Nanomaterials in Biomedical Engineering



Herein, the working principle, design, and classification of piezoelectric nanomaterials are systematically reviewed. The latest progress of piezoelectric nanomaterials and their applications in tissue regeneration, antitumor/antibacterial therapy, cell force detection, controlled drug release, and pathological/physiological parameter monitoring are highlighted. The summary of biomedical applications of piezoelectric nanomaterials will inspire novel diagnostic and therapeutic strategies in the future.

Research Trends of Piezoelectric Nanomaterials in Biomedical Engineering

Jianying Ji, Chunyu Yang, Yizhu Shan, Mingjun Sun, Xi Cui, Lingling Xu, Shiyuan Liang, Tong Li, Yijie Fan, Dan Luo,* and Zhou Li*

Piezoelectric nanomaterials are functional materials that hold a great promise for the nanoscale conversion of mechanical energy and electrical signals. Owing to their excellent electromechanical dependence, catalytic activity, and response sensitivity, piezoelectric nanomaterials are widely used in energy harvesting, sensors, actuators, resonators, and medical detectors. Nano-piezoelectric materials exhibit unique electrical and chemical activities in the field of biomedical engineering, such as disease diagnosis and treatment. The working principles, device-design mechanics, and classification of piezoelectric nanomaterials are systematically reviewed. Then, the recent advances in piezoelectric nanomaterials and their applications in tissue regeneration, antitumor/antibacterial therapy, cell force detection, controlled drug release, and pathological/physiological parameter monitoring are highlighted. Finally, the perspectives on the development of future smart piezoelectric nanomaterials, and how they can serve as a building block to inspire and impact the development of novel diagnosis and treatment applications, are presented.

are displaced and appear on the upper and lower surfaces of the material.^[2] The charge density is proportional to the applied mechanical force, and the phenomenon of transforming mechanical energy into electrical energy is called the positive piezoelectric effect. In contrast, when the piezoelectric material is subjected to an external electric field, the positive and negative charge centers inside the crystal are displaced, resulting in the deformation of the crystal. The inverse piezoelectric effect is a process in which electrical energy is transformed into mechanical energy.^[3] These two effects are collectively referred to as piezoelectric effects, and materials with piezoelectric effects are defined as piezoelectric materials. The development of piezoelectric materials has undergone four stages: piezoelectric crystals,^[4] piezoelectric ceramics,^[5] piezoelectric polymers,^[6] and piezoelectric composites.^[7] The earliest developed piezoelectric crystals are now only used in high-precision sensors owing to their high cost. Subsequently, piezoelectric ceramics have emergence and have gradually replaced piezoelectric crystals. The application of these materials realized has led to the expansion of their applications. In recent years, researchers have found that natural materials such as wood^[8] and bone^[9] also exhibit piezoelectricity. Recently, piezoelectric ceramics and piezoelectric

1. Introduction

Piezoelectric materials are useful materials that can achieve the mutual conversion of mechanical and electrical energy. Its earliest research can be traced back to 1880, when the French physicists P. Curie and J. Curie discovered the piezoelectric effect.^[1] When pressure, tangential force, and tension are applied, the positive and negative charges inside the piezoelectric material

J. Ji, C. Yang, Y. Shan, M. Sun, X. Cui, L. Xu, S. Liang, T. Li, Y. Fan, D. Luo, Z. Li
Institute of Nanoenergy and Nanosystems
Chinese Academy of Science
Beijing 101400, China
E-mail: luodan@binn.cas.cn; zli@binn.cas.cn

J. Ji, T. Li, Z. Li
Center on Nanoenergy Research
School of Physical Science and Technology
Guangxi University
Nanning 530004, China

 The ORCID identification number(s) for the author(s) of this article can be found under <https://doi.org/10.1002/anbr.202200088>.

© 2022 The Authors. Advanced NanoBiomed Research published by Wiley-VCH GmbH. This is an open access article under the terms of the Creative Commons Attribution License, which permits use, distribution and reproduction in any medium, provided the original work is properly cited.

DOI: 10.1002/anbr.202200088

C. Yang, M. Sun
State Key Laboratory of Heavy Oil Processing
College of New Energy and Materials
Beijing Key Laboratory of Biogas Upgrading Utilization
China University of Petroleum (Beijing)
Beijing 102249, China

C. Yang, M. Sun
Institute of Engineering Medicine
School of Life Science
Beijing Institute of Technology
Beijing 100081, China

L. Xu
National Center for Nanoscience and Technology
Chinese Academy of Sciences
Beijing 100190, China

D. Luo, Z. Li
School of Nanoscience and Technology
University of Chinese Academy of Sciences
Beijing 100049, China

polymers have been the most researched and frequently utilized piezoelectric materials.

Various piezoelectric nanomaterials have emerged in the past few years owing to the rapid development of electronic components for ultraminiaturization, high intelligence, and high integration and are used for sensing, electrochemistry, energy harvesting, electronics, and therapy.^[10] To date, the prepared piezoelectric nanomaterials include but are not limited to zinc oxide (ZnO) nanowires (NWs),^[11] PMN-PT NWs,^[12] NaNbO₃ NWs,^[13] zinc sulfide (ZnS) nanobelts (NBs),^[14] barium titanate (BaTiO₃) nanoparticles (NPs),^[15] lead zirconate titanate (PZT) nanofilms,^[16] polyvinylidene fluoride (PVDF) nanofibers (NFs),^[17] and others. Nanostructures often exhibit physical properties superior to those of materials.^[18] For example, the piezoelectric coefficient of ZnO bulk material is 9.9 pm V⁻¹ while that of ZnO nanoribbons is as high as 26.7 pm V⁻¹.^[19] As the NP diameter decreases, the surface area and specific surface area of the material significantly increase, accompanied by a rapid increase in the number of surface atoms.^[20] The large number of defects and dangling bonds on the surface of nanoscale materials eventually leads to enhanced surface atomic activity, which in turn leads to changes in the transport and configuration of surface atoms, as well as the spin conformation and electron energy spectrum of the surface electrons.

Bioelectricity is an indispensable regulator of growth and development in living systems.^[21] Endogenous electric fields (EFs) play a crucial role in a wide variety of physiological processes, such as embryonic development,^[22] tissue regeneration,^[23] cell migration,^[24] and fracture recovery.^[25] However, the complexity of patients and the inconvenience of electrotherapy methods have triggered the development of piezoelectric biomaterials with built-in electrical signaling capabilities. In a physiological environment, piezoelectric nanocrystals undergo displacement of intracellular atomic positions under mechanical stress, resulting in the loss of symmetry centers and the accumulation of charges through ordered dipole distributions. The resulting electrical signals can act directly on living systems or indirectly through catalytic reactions.^[26] Many piezoelectric biomaterials have been investigated for various biomedical engineering applications.^[27] This article systematically reviews the piezoelectric mechanism, classification, biological effects, and applications of piezoelectric nanomaterials and their applications in tissue engineering, antitumor/antibacterial therapy, cell force detection, controlled drug release, and physiological signal detection. This review also describes the future prospects of piezoelectric nanomaterials in biomedical engineering.

2. Classification and Functions of Nanoscale Piezoelectric Materials

2.1. Principle of the Piezoelectric Effect

Piezoelectric materials polarize under an applied stress, which is defined as the direct piezoelectric effect (Figure 1a). d_{33} , a parameter used to characterize the piezoelectric properties of materials, is a measure of the charge generated by the application of a mechanical load. The larger the d_{33} value of the material, the

higher is its piezoelectricity.^[28] The direct piezoelectric effect can be calculated by using Equation (1)

$$D = d \times T + e \times E \quad (1)$$

where D denotes the displacement; d is the piezoelectric coefficient; T is the applied mechanical stress; e is the dielectric constant of the material; and E represents the field.

The reverse piezoelectric effect can be expressed as Equation (2)

$$X = s \times T + d \times E \quad (2)$$

where X is the strain and s refers to mechanical compliance.^[29]

The piezoelectric effect was discovered by scientists more than 100 years ago,^[30] and the mechanism underlying this effect has only recently been revealed. The most common material with a piezoelectric effect is ZnO with a wurtzite structure, which can be regarded as a crystal formed by multiple tetrahedra with Zn²⁺ and O²⁻ as vertices stacked along the C-axis (Figure 1b). In the absence of an external force, it is electrically neutral because the cation and anion charge centers overlap. When an external force is applied, the positive and negative charge centers are separated, resulting in dipoles (Figure 1b).^[31] Piezoelectric polymers are generally crystalline polymers with piezoelectric effect crystal regions. There is no overwhelmingly convincing general theory for describing piezoelectricity in polymers. One of the reasons for the complexity of polymer systems is their semi-crystalline structure. Polymers are networks of long-chain molecules, and regions of these polymer chains can form small crystallites. However, these regions are surrounded by an amorphous matrix of the remaining polymer chains. Therefore, crystallinity plays a key role in the piezoelectric properties of polymers. In contrast, the β phase of the crystalline portion is an important factor that determines piezoelectricity. The β phase has an all trans conformation (TTTT), so the polymer chains of the β phase are aligned and stacked in the same direction as the polarization, resulting in piezoelectricity.^[6] In addition to traditional inorganic crystals, researchers have recently discovered that piezoelectricity exists in many natural tissues in living organisms, such as wood,^[8] bone,^[9] tendon,^[32] and deoxyribonucleic acid (DNA).^[33] This indicates that the piezoelectric effect may also play an important role in the growth, development, and maintenance of physiological functions.^[34] These findings suggest that the use of synthetic piezoelectric nanomaterials is expected to modulate pathophysiological processes, showing excellent application prospects in the field of biomedical engineering.^[35]

2.2. Classification of Nanomaterials with Piezoelectric Effect

Piezoelectric materials are generally divided into three categories, namely, inorganic, organic, and composite. For piezoelectric nanomaterials that can be applied in the biomedical field, research has mainly focused on piezoelectric ceramics, third-generation semiconductors, piezoelectric polymers, piezoelectric biomaterials, and asymmetric materials based on atomic interface engineering.

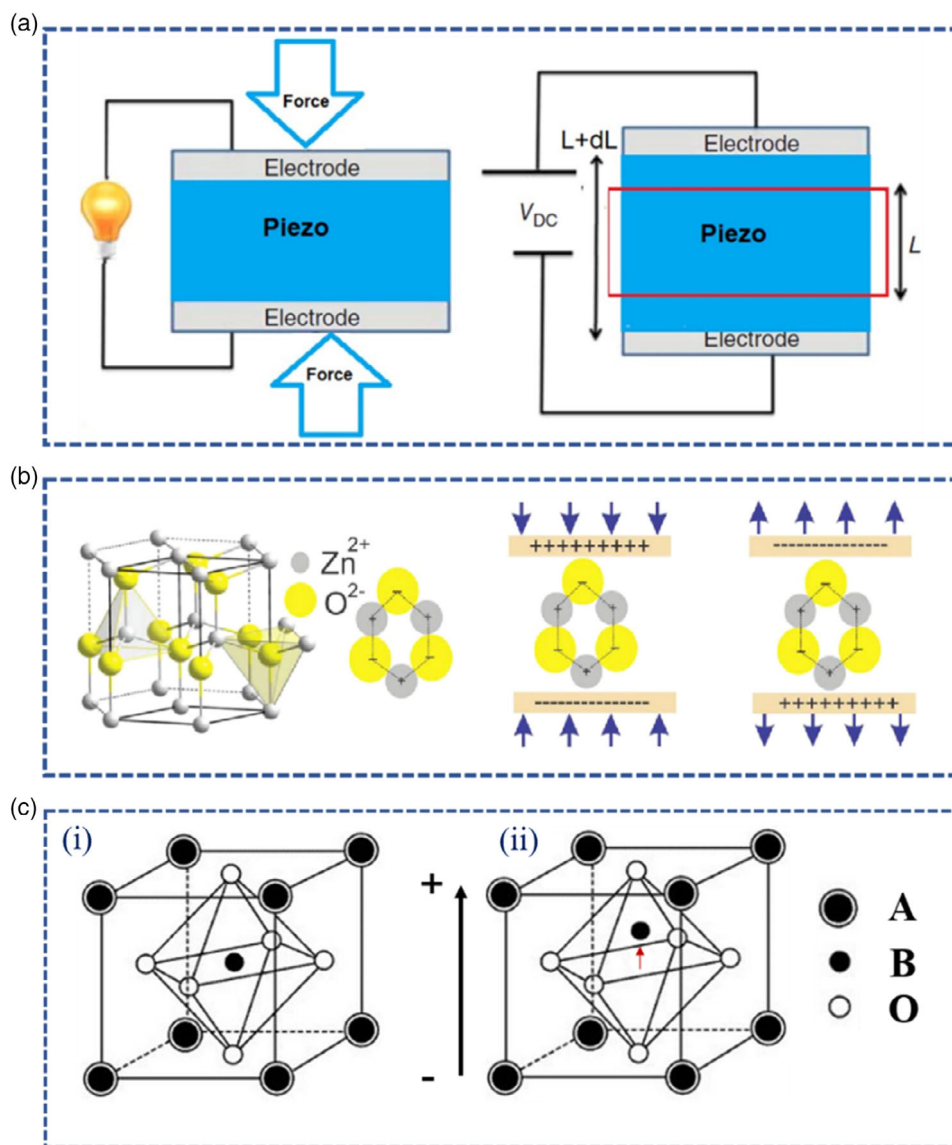


Figure 1. a) Schematic diagram of direct and reverse piezoelectric effects. b) ZnO fiber-zinc ore structural model, piezoelectric potential in compression and tensile mode. c) Perovskite structures in paraelectric i) and ferroelectric ii) phases. Reproduced with permission.^[31] Copyright 2022, Elsevier.

2.2.1. Piezoelectric Ceramics

BaTiO₃ ceramics were first discovered during World War II. The research showed that after removing the direct current, the remanent polarization of the BaTiO₃ ceramics was still retained and preferentially aligned along the electric field direction. Thus, the piezoelectric effect of the ceramics was discovered and piezoelectric ceramics were born. In 1955, Jaffe et al. found that lead zirconate titanate (PZT) ceramics possessed a better piezoelectric effect than BaTiO₃ ceramics, and this discovery led to the development of lead-based piezoelectric ceramics, which have played a pivotal role in piezoelectric materials until now.^[36] However, lead oxide (PbO), the main raw material in the lead-based ceramics, is harmful to human health and the ecological environment.^[37] Lead-free ceramics have recently received extensive attention

from researchers and are expected to replace lead-based piezoelectric ceramics.^[37] Current research on lead-free piezoelectric ceramics mainly includes the following three structures, namely, perovskite,^[38] bismuth layered,^[39] and tungsten bronze structures.^[40] As the most common piezoelectric ceramic structure, perovskite structure exists in both lead-based (such as PZT and PbTiO₃) and lead-free (such as BaTiO₃, KNN, and KNbO₃) piezoelectric ceramics.^[41] Figure 1c-i shows a typical paraelectric phase perovskite structure unit cell, and its general structural formula can be represented by ABO₃. Among them, A atoms and O atoms with larger atomic radii occupy the vertices and face centers of the hexahedron, respectively, whereas B atoms with smaller atomic radius occupy the center of the entire structure. Under normal conditions, the entire system is centrosymmetric with the centers of positive and negative charges

overlapping, so there is no polarization and no piezoelectricity. However, when the temperature drops below the Curie temperature (T_c), the position of the B atom changes, causing the center of positive and negative charge to shift (Figure 1c-ii).^[20,42] Consequently, the perovskite structure undergoes spontaneous polarization, resulting in the generation of ferroelectricity and piezoelectricity. Tungsten bronze structural compounds are another large class of piezoelectric materials that exhibit excellent ferroelectricity.^[39] These crystals exist in $[\text{BO}_6]$ oxygen octahedrons (B = Nb⁵⁺, Ta⁵⁺, W⁶⁺, and others), forming a skeleton with apex angles, thereby stacking into a tungsten bronze structure. Although tungsten bronze structural compounds, such as perovskite structures, are composed of $[\text{BO}_6]$ oxygen octahedra as basic units, the final structures contain not only octahedral voids but also 12-hedral and 15-hedral voids owing to the different stacking methods.^[40] The valence band of bismuth layered-structure materials is formed by the hybridization of the Bi 6s and O 2p orbitals. This strong interaction reduces the symmetry of the structure and manifests in the form of dipoles, resulting in dipole-related properties, including piezoelectric properties.

2.2.2. Third-Generation Semiconductors

Most traditional piezoelectric materials are insulators. Third-generation semiconductor materials, such as gallium nitride (GaN), silicon carbide (SiC), and ZnO, have started to appear in the twenty-first century. Third-generation semiconductor materials have a hexagonally symmetric wurtzite crystal structures. The atoms in the unit cell are hexagonally densely packed based on the tetrahedral structure, and the double-layer atoms are periodically stacked along the (0001) direction (Figure 1b). Wurtzite has a polar structure and good piezoelectric and ferroelectric properties. The wurtzite crystal structure has no axial symmetry because of the distinct charge properties of the different atoms in the crystal form. In the 1960s, Maruska and Tietjen took the lead in successfully preparing the first GaN single crystal using vapor-phase epitaxy and subsequently reported its semiconductor optical properties.^[43] In the 1980s, Amano et al. successfully prepared high-quality GaN single crystals with a simple sandwich structure, which significantly reduced the intrinsic electron doping concentration and greatly improved the electron mobility.^[44] Additionally, the development of *p*-type doping technology has promoted research on GaN. Research on III-V nitrides prompted a gradual increase in the exploration of ZnO. ZnO, as compared to GaN, has a high exciton binding energy of 60 meV and a large forbidden band width of 3.4 eV, which gives ZnO excellent advantages in high-temperature, high-efficiency, and low-threshold short-wavelength laser emission.^[45] Another unique feature of ZnO is that it enables the growth of various low-dimensional nanostructures such as NWs, nanoribbons, nanorings, NFs, and nanotubes.^[46] In 2006, Wang first demonstrated a piezoelectric nanogenerator (PENG) using ZnO NWs and realized the conversion of mechanical energy into electricity, marking the arrival of the nanoenergy era.^[47] The PENG uses the mechanical stress-induced piezoelectric potential to drive a closed-loop current, and the bent NWs serve as an external power source. Third-generation semiconductors benefit from their high-voltage

electroactivity, fine nanostructures, and good biocompatibility,^[48] thereby promoting the application of piezoelectric nanomaterials in biomedicine.^[49]

2.2.3. Piezoelectric Polymer

Piezoelectric polymers are long-chain carbon-based materials with piezoelectric effects, such as PVDF,^[17,50] nylon-11 (PA-11),^[51] and PVDF-trifluoroethylene (PVDF-TrFE).^[52] These polymers are typically semicrystalline materials with crystalline regions embedded in an amorphous matrix. During manufacturing, they usually have a nonpolarized phase after cooling from the melt. To impart piezoelectric properties to these polymers, the apolar phase must be converted to the polar phase using uniaxial or biaxial stretching, polarity must be induced using solution casting, and the dipoles must be aligned using electrode or corona polarization treatment.^[53] Piezoelectric polymers typically have the advantages of high flexibility, easy film formation, good mechanical properties, and ease of large-scale integration. As a representative piezoelectric polymer, PVDF is a semicrystalline polymer with five different crystalline phases, among which the β phase is most important because of its large polarizability and high-voltage electrical sensitivity. Researchers have employed various strategies to obtain PVDFs with higher β phase ratios, such as in situ polarization, thermal stretching, and high electric field induction.^[54] The advantages of PVDF-TrFE, as compared to PVDF, lie in the directional T_c and a larger electromechanical coupling coefficient. The piezoelectric constants of piezoelectric polymers are significantly smaller than those of piezoelectric ceramics, which limits their application in energy harvesting. However, piezoelectric polymers are widely used in flexible medical devices and tissue engineering scaffolds because of their structural flexibility, ease of processing, good chemical stability, excellent biocompatibility, and mechanical strength. Liu et al. fabricated continuous polyvinylidene fluoride (PVDF) sheets with a high β -phase content using melt extrusion-calendering technology and assembled PVDF-based PENG for the real-time monitoring of various human movements.^[55] Eom et al. fabricated piezoelectric PA-11 delta-phase crystalline thin films using humidity-conditioned casting and a subsequent melt quenching process, which exhibited excellent piezoelectric properties under external vertical pressure and could be used as a Morse code detector.^[56] Yuan et al. reported a three-dimensional (3D)-printed PVDF-TrFE piezoelectric film (ID-TPPF) coated with a pair of interdigitated electrodes, which generated a stable peak voltage of 73.5 V under a dynamic compressive stress of 50 kPa at 1 Hz, corresponding to a pressure sensitivity of 1.47 V kPa⁻¹. Its performance was 14.7 times and 3.6 times that of conventional thickness-polarized and in-plane polarized PVDF-TrFE films, respectively. When the load was 3 M Ω , the load power remained at 207 $\mu\text{W cm}^{-2}$, even without any charging capacitors, which is sufficient to instantly power eight light-emitting diodes connected in series. This study demonstrated that 3D-printed ID-TPPF shows good potential for future self-powered tactile sensors and artificial skin applications.^[57]

2.2.4. Piezoelectric Biomaterials

The piezoelectric effect of organic piezoelectric materials is caused by the asymmetry of their molecular structure and orientation.^[58] Because biomaterials often have highly organized structures with minimal symmetry and no inversion centers, linear electromechanical coupling is a characteristic of many biomolecules. Since it was discovered that natural materials, such as cellulose^[59] and collagen,^[60] have a piezoelectric effect, an increasing number of biological materials have also been revealed to have this property. The currently known piezoelectric biomaterials can be divided into two categories, namely, piezoelectric biomolecules and piezoelectric biotissues. Common piezoelectric biomolecules include cellulose, amino acids, peptides, proteins, and DNA, whereas common piezoelectric biological tissues include bone, hair, and epidermis. Wang et al. presented a wafer-scale method to produce piezoelectric biomaterial thin films using *ong-glycine* crystals.^[61] The crystalline glycine layer self-assembled and automatically aligned between the two polyvinyl alcohol (PVA) thin films in the sandwich-like structure of the thin film. The heterostructured glycine-PVA films, as compared to pure glycine crystals, exhibited piezoelectric coefficients of 5.3 pC N^{-1} or $157.5 \times 10^{-3} \text{ Vm N}^{-1}$, and their mechanical flexibility was improved by nearly an order of magnitude. Yang et al. reported a van der Waals exfoliation (vdWE) approach to create ultrathin films with the thickness of the effective piezoelectric domain using the weak van der Waals interaction in the layered structure of the small intestine submucosa (SIS).^[62] They discovered that the SIS produced from the collagen fibril exhibited piezoelectric properties with piezoelectric coefficients up to 4.1 pm V^{-1} and an in-plane polarization direction parallel to the fibril axis. Scientists also presented a biosensor based on an SIS film that had undergone vdWE processing and had an in-plane electrode. This biosensor generated open-circuit voltages of approximately 250 mV under cantilever-shaking conditions. The vdWE approach is promising for the quick and easy preparation of biosensors and soft-tissue ultrathin films. Piezoelectric biomaterials have excellent biocompatibility, reliability, and environmental sustainability and, thus, have promising application prospects in biomedical engineering.

2.2.5. Asymmetric Materials Based on Atomic Interface Engineering

The early research on piezoelectric materials was limited to macroscopic bulk materials. However, when the scale of the material in a certain dimension reaches the nanometer or subnanometer scale, the traditionally considered nonpiezoelectric material produces piezoelectricity. The surface effect caused by a high specific surface area is one of the most important structural features of nanomaterials. For macroscopic bulk materials, the proportion of surface atoms in the total atoms is very low; therefore, the influence of the surface effects is too small to be considered. As the size of the material decreases, the proportion of surface atoms in the total number of atoms increases sharply. The presence of a large number of defects and dangling bonds on the surface causes the electrical, magnetic, optical, and catalytic properties of nanomaterials to be significantly different from those of

macroscopic bulk materials. Some two-dimensional (2D) layered materials, such as transition metal sulfides (MoS_2 , MoSe_2 , and WTe_2), exhibit different crystallographic spatial symmetries with varying layer thicknesses. Their 3D bulk form is centrosymmetric; however, when its thickness is reduced to just one atomic layer, it becomes noncentrosymmetric.^[63] Therefore, the monolayer of molybdenum disulfide (MoS_2) has a piezoelectric effect, which is not observed in 3D bulk materials. In 2014, Wang et al. studied the piezoelectric properties of 2D MoS_2 for the first time.^[64] By applying a tensile force of 0.53% to the monolayer sheet, a peak voltage of 15 mV and peak current output of 20 pA were generated, corresponding to an energy density of 2 mW M^{-2} and a mechanical–electrical energy conversion rate of 5.08%. The current/voltage output reversed after the tension direction was rotated by 90° , which was consistent with the theoretical predictions. Transport measurements showed a strong piezoelectric effect in monolayer MoS_2 , which was absent in bilayer and bulk MoS_2 .

2.3. Principles of Piezoelectric Nanomaterials Acting on Living Systems

Piezoelectric nanomaterials generally affect biological systems via two main pathways, namely, the direct electrical stimulation of the organism, which affects the growth, development, proliferation, and other behaviors of cells by affecting the ions and electro-sensitive proteins of cells; and the generation of reactive oxygen species (ROS), which is promoted by piezoelectrically polarized charges. ROS leads to apoptosis through oxidative stress and mediated DNA damage, making it widely used in anti-tumor and pathogen clearance.

2.3.1. Direct Electrical Stimulation

Electrical stimulation as a noninvasive and nonpharmacological physical stimulus has a wide range of biomedical effects. It has been used for muscle rehabilitation, movement/consciousness disorders treatment, drug delivery, and wound healing. At the molecular level, ES facilitates the transport of biomolecules through biofilm by electrophoresis and electropenetration. At the subcellular level, electrical stimulation also interacts with the cytoskeleton, membrane proteins, ion channels, and various intracellular organelles, thereby altering cellular activities and functions, such as contraction, migration, orientation, and proliferation (**Figure 2**).

The basic mechanisms underlying cellular response to electrical stimulation can be summarized as follows: 1) electrical stimulation disrupts the order of structural water on the extracellular surface. This damage causes cells to lose their gel structures and release a large amount of trapped Ca^{2+} ions. Moreover, it also leads to an influx of Na^+ ions and outflow of K^+ ions. The flow of ions changes the volume and membrane potential of cells. 2) Electroosmosis not only accelerates the transmembrane delivery of drugs but also generates a hydrodynamic drag force to redirect cells due to the difference in the adsorbed aqueous shell of Na^+ and K^+ ions across the cell membrane. Therefore, in the presence of an electric field, an external hydrodynamic drag force acting on the cells is generated, which affects the migration of

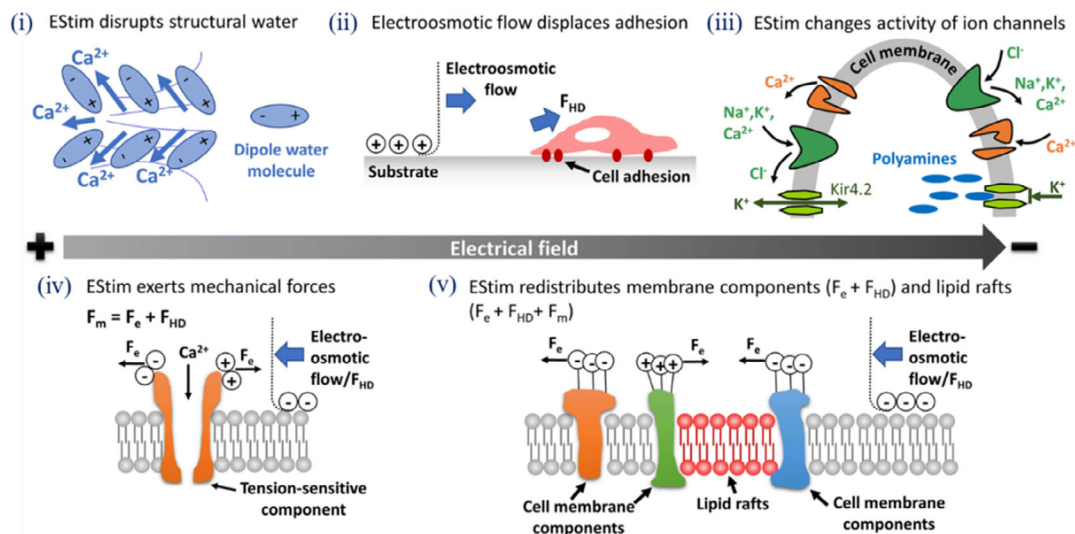


Figure 2. The basic physical effect of estim on cells: i) destruction of the structured aqueous layer. ii) Hydrodynamic resistance exerted by electroosmotic currents on the surface of the cell can make the adhesion of cell. iii) Polarization of cells by estim can alter the switching of electromotive force and the switching of ion channels. iv) Electroosmotic force arouse force sensor. v) The redistribution of membrane composition and lipid rafts. Reproduced with permission.^[65] Copyright 2020, American Association for the Advancement of Science.

cells and the transport of intracellular biomolecules. 3) The presence of an electric field creates an asymmetric ion flow. The cells are polarized on the anode side while depolarizing the cathode side. Different cell surface membrane potentials can open ion channels and generate an asymmetric flow of ions, ultimately affecting various cellular behaviors. 4) The electroosmotic and electrostatic forces generated by the electric field can also act on tension-sensitive components on the cell surface, thereby affecting gene expression and downstream signaling pathways, ultimately affecting cell proliferation, growth, and migration. 5) The electric field and the force generated by the electric field lead to the redistribution of membrane components and lipid rafts, thereby further polarizing the integrin, caveolin, and other components on the cell membrane. Integrins can affect cell migration, and this redistribution can affect intracellular signaling and intercellular communication.^[65]

2.3.2. Free Radicals Based on the Piezoelectric Effect

In addition to the direct application of electrical stimulation, external mechanical forces can separate the charge carriers of piezoelectric nanomaterials and generate ROS that act on biological systems.^[66] Ultrasound waves, a type of mechanical wave, can produce a cavitation effect. During the formation, growth, and rupture of vacuoles, the continuously generated microscopic severe periodic pressure is an ideal energy source for driving piezoelectric nanomaterials. Piezoelectric materials establish dynamic built-in EFs under acoustic vibrations, making electron and hole pairs continuous separate for piezoelectric catalytic redox reactions, thereby generating reactive oxygen species (ROS), such as toxic hydroxyl groups ($\bullet\text{OH}$) and superoxide radicals ($\bullet\text{O}^{2-}$). The above-mentioned therapeutic strategy for generating ROS using piezoelectric materials is called sonodynamic therapy (SDT). Because ultrasound can penetrate deep tissue,

photodynamic therapy (PDT) can eliminate deep tumors in situ and effectively remove pathogens. Owing to the nanosize effect, piezoelectric nanomaterials generally exhibit better piezoelectric effects than macroscopic bulk structures.^[48]

3. Biomedical Engineering Applications of Piezoelectric Nanomaterials

3.1. Tissue Regeneration

Tissue engineering uses regeneration to fix or replace damaged tissues and organs.^[28] A typical tissue engineering research procedure involves first extracting cells from a donor,^[67] then culturing them in vitro, usually on a scaffold with growth-promoting factors, and finally transplanting the cultured tissue back into the host.^[68] Electrical stimulation can cause various changes in the genes and phenotypes of cells, thereby affecting cell growth, attachment, proliferation, and development. Cafarelli et al. systematically characterized the acoustics of agarose, polyacrylamide, and polydimethylsiloxane doped with various quantities of BaTiO_3 NPs. They confirmed that the proliferation of human fibroblasts was correlated with precise ultrasound doses. The nanomaterials could provide an accurate nanoscale morphology, which was conducive to cell attachment and growth. This research has groundbreaking implications for tissue simulation models in tissue engineering and regenerative medicine.^[69] Therefore, it is of great significance to develop piezoelectric nanomaterials that can provide electrical stimulation for tissue regeneration.^[70]

3.1.1. Bone Regeneration

Bone regeneration is a complex process that involves the reconstruction of bone structure and function. Implanted scaffolds are

required as supports when the bone defect exceeds a critical size. Nanomaterials can mimic the characteristics of bone at the micro/nanoscale and modulate the behavior of cells through their surface morphology, chemical composition, and physical properties.^[71] A variety of nanomaterials have been developed for bone repair. Giada et al. used piezoelectric poly(vinylidene fluoride-trifluoroethylene) (P(VDF-TrFE))/boron nitride (BN) nanotube composite membranes to stimulate the development of human SaOS-2 osteoblast-like cells. This study verified the promoting effect of membrane mechano-electrical transduction on osteogenic differentiation by studying the cellular response after ultrasound stimulation, which is of great significance for bone tissue engineering.^[72] Owing to the asymmetric structure of the collagen that constitutes bone, natural bone is piezoelectric and can regulate bone growth and fracture healing through electrical signals. Therefore, nanomaterials with piezoelectric properties are expected to have promising prospects for bone regeneration.

Three categories of piezoelectric materials are currently used for osteogenesis, namely, piezoelectric polymers, lead-free piezoelectric ceramic materials, and ceramic matrix composites. The bone repair capacity can be further enhanced by combining piezoelectric nanomaterials with traditional bone grafting materials.^[73] Most piezoelectric materials used for bone regeneration, such as BaTiO₃, cannot be 3D printed, and their mechanical properties are not as good as those of titanium alloys. An effective method is to coating the piezoelectric material on the stent, which can retain the load-bearing nature of the scaffold while recovering the physiological electro-microenvironment of the piezoelectric material at the bone defect. Liu et al. coated barium carbonate, a piezoelectric substance that has been shown using cell tests to be advantageous for the proliferation, motility, and osteogenic differentiation of mesenchymal stem cells, on a porous titanium alloy that could be 3D printed. Spinal fusion model experiments in sheep demonstrated that the piezoelectric coating significantly enhanced bone regeneration and vascularization.^[74] Polyvinylidene difluoride (PVDF) is also a biocompatible piezoelectric polymer, Cong et al. coated PVDF on pure commercial titanium plates to increase its piezoelectric properties, but the hydrophobic properties of the PVDF were not conducive to the deposition of bone apatite. To improve the situation, Cong et al. doped hydroxyapatite (HA) in the PVDF, and cell experiments demonstrated that the material was capable of reducing the contact angle and was completely covered with apatite in the simulation solution. This shows that the material has great value in bone repair applications.^[75]

Although exogenous electrical stimulation can theoretically promote bone regeneration, the use of synthetic piezoelectric materials often leads to biotoxicity and degradability concerns. To solve this problem, Vignesh et al. developed whitlovitte (WH) NPs (Figure 3a),^[25] which exhibited moderate bioabsorbability, as compared to HA and tricalcium phosphate. WH NPs can generate electrical signals similar to those of native tissue when irradiated with low-intensity pulsed ultrasound. According to the in vitro studies, WH NPs effectively aided in the proliferation and differentiation of mouse embryonic osteoblasts, according to in vitro research. The mechanisms by which piezoelectric WH NPs enhance osteogenic differentiation were also assessed by mRNA expression level analysis using real-time quantitative

polymerase chain reaction (QRT-PCR). The expression of transient receptor potential vanilloid 4 (TRPV4) and piezo type mechanosensitive ion channel component 1 (PIEZO1) increased, the associated downstream signaling pathways were activated, and this ultimately promoted osteogenic differentiation by increasing the expression of Cox2 and CREB in osteoblasts.

The surface of the bone defects can be quickly covered by the periosteum, which promotes the migration of osteoblasts and enables rapid closure and growth of the defect area.^[76] However, it is difficult to regenerate new bone when the bone defect reaches a critical size because its surface is not fully covered by the periosteum. Zhao et al. designed a novel PVDF-TrFE-bioactive glasses micro-nano particles (PVFT-BGM) scaffold that combined piezoelectric polymers and bioactive glass NFs to simulate the periosteal structure and bone microenvironment (Figure 3b).^[76] Piezoelectric polymers mimicked the electrical environment of bone to induce osteoblast migration, and bioglass NFs released Ca²⁺, phosphorus ions (P⁴⁺), and other mineral ions. Further mechanistic studies confirmed that PVFT-BGM promoted osteogenesis by activating Ca²⁺-sensitive receptors (CaSR) in osteoblasts and affecting downstream signaling pathways. The scaffold was able to promote the growth, proliferation, and differentiation of bone marrow stem cells, while the formation of periosteum-like tissue and bone regeneration were observed.

Whether the positively charged surface or the negatively charged surface is beneficial for promoting osteogenic differentiation is still controversial. Because GaN and AlGaN are wurtzite structures with different spontaneous polarizations in opposite directions, the heterostructure of GaN and AlGaN can be adjusted by adjusting the direction and magnitude of the spontaneous and piezoelectric polarizations to finally adjust the surface charge. Zhang et al. designed two piezoelectric heterostructure materials with opposite surface polarities: negatively charged Ga-GaN/AlGaN and positively charged N-GaN/AlGaN (Figure 3c).^[77] It was experimentally confirmed that Ga-GaN/AlGaN with negative surface charge significantly promoted the attachment, osteogenesis differentiation, diffusion, and recruitment of bone mesenchymal stem cells. Based on this mechanism, it was found that bone morphogenetic protein-6 (BMP6) may play the role as an electrosensitive protein in the early stage of osteogenic differentiation, but further research is needed to elucidate the underlying mechanisms.

3.1.2. Nerve Regeneration

With the high incidence of traffic accidents and industrial accidents, peripheral nerve injury has become a common serious traumatic disease, with an annual incidence of 20 out of 100 000 people every year. Usually, minor nerve injury has the ability to recover on its own, but when the injury is more serious, medical intervention is required. In clinical practice, autologous nerve grafts are often used to bridge the proximal and distal ends of the defect, so as to realize the recovery of the sensory and function of the injury. However, autologous transplantation inevitably has the problems of scarcity of resources, mismatched size, and damage to the autologous body. Therefore, artificial nerve guides can be used as an alternative, which can promote nerve repair by

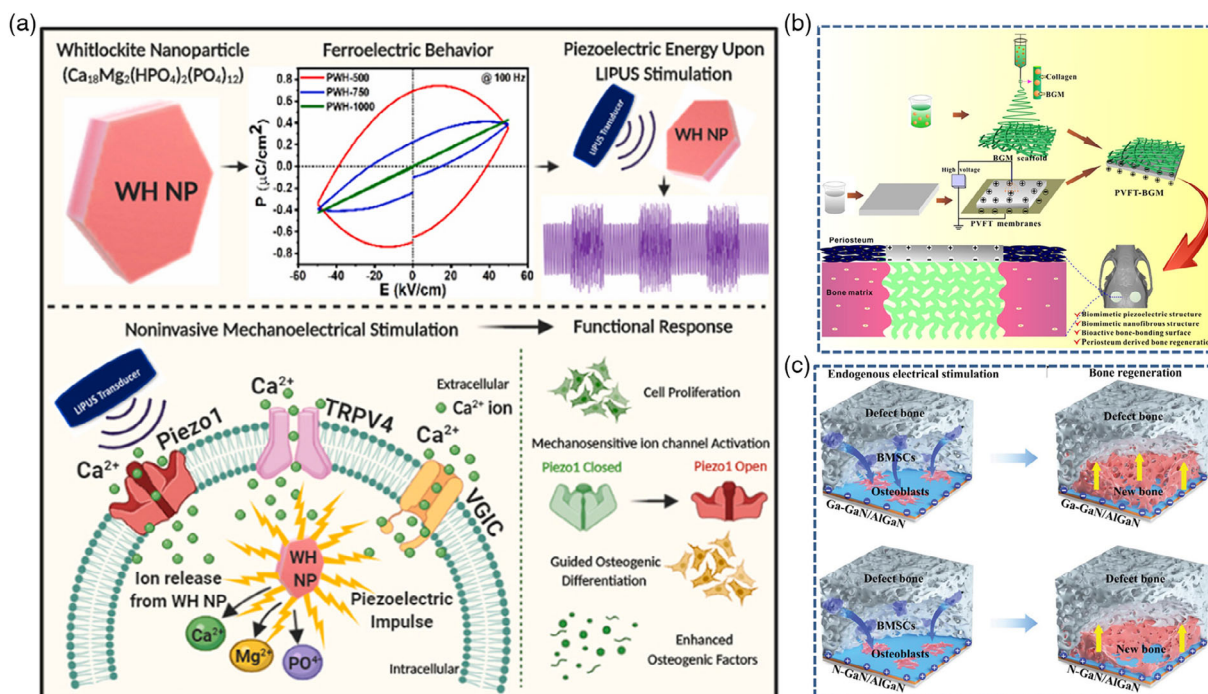


Figure 3. a) Synthesis of piezoelectric WHNPs, as well as noninvasive mechanical electrical stimulation of WHNPs on pre-osteoblast cells and their responses. b) Synthesis of PVFT-BGM scaffolds and possible mechanisms by which PVFT-BGM scaffolds promote osteogenesis. c) GaN/AlGaN films promote the process of bone regeneration by inducing endogenous electrical stimulation. a) Reproduced with permission.^[25] Copyright 2021, Elsevier. b) Reproduced with permission.^[76] Copyright 2020, Elsevier. c) Reproduced with permission.^[77] Copyright 2021, WILEY-VCH.

providing electrical conductivity, mechanical support, and a biomimetic microenvironment to damaged nerves. Piezoelectric materials, as compared to traditional conductive materials, such as polypyrrole, graphene, and gold NPs (AuNPs), are very promising because they do not require connection to an external power source.^[78]

Typically constructed of biocompatible polymers, such as polycaprolactone (PCL) and neural catheters (NCCs), mechanically close the space between two nerve stumps while directing the growth of neurites from proximal to distal. BN is a 2D piezoelectric ceramic material with high biocompatibility and stable chemical properties. Qian et al. fabricated a functionalized interface of BN nanosheets (BNNS) (Figure 4a).^[79] This interface reduced the damage caused by oxidative stress by increasing the level of antioxidants under the action of ultrasound and achieved immune homeostasis by regulating the level of ROS, finally promoting the growth, development, and proliferation of Schwann cells and accelerating remyelination and axon growth under mechanical stimulation. The BNNS functional interface enables the treatment of nerve injuries through multiple aspects, namely, restoring the bioelectric signals in the injured nerve, generating an appropriate concentration of ROS, realizing nutrient supply to injured nerves through angiogenesis, and ultimately achieving the purpose of functional recovery.

Qian et al. developed a ZnO/PCL (polycaprolactone) polymer scaffold made by a 3D injectable multilayer biofabrication method. The PCL component is a commonly used polymer matrix material for making nerve conduits, with suitable

stiffness and the slow degradation rate that is suitable for neuron regeneration. ZnO is an antibacterial, biocompatible, and environmentally friendly piezoelectric material. Experimental evidence showed increased expression of nerve growth factor and vascular endothelial growth factor, indicating that the scaffold could be effective in the attachment and proliferation of Schwann cell and angiogenesis. Meanwhile, the injured peripheral nerves in mice were able to recover within 18 weeks without significant biological toxicity (Figure 4b).^[80] Similarly, Mao et al. also designed a PCL/ZnO NF (PZNF) piezoelectric nerve conduit (Figure 4c).^[81] Regarding the controversial biological toxicity of ZnO, the toxicity was controlled within an acceptable range by adjusting the concentration. PZNF achieved repair of mouse sciatic nerve injury within four weeks. The time was controlled within the peak time of the repair event of the injury response, and the apoptosis of Schwann cells and fibroblasts was avoided. The study also investigated the promoting mechanism of sciatic nerve regeneration by PZNF, which involved the activation of growth factor receptor-bound protein-2 (GRB2), which might act as an electrosensitive protein to affect multiple downstream signaling pathways and promote peripheral nerve regeneration.

3.1.3. Wound Healing

Hemostasis, inflammation, proliferation, and dermal remodeling are the four stages of wound healing. Chronic and nonhealing wounds are caused by factors such as infection, inflammation,

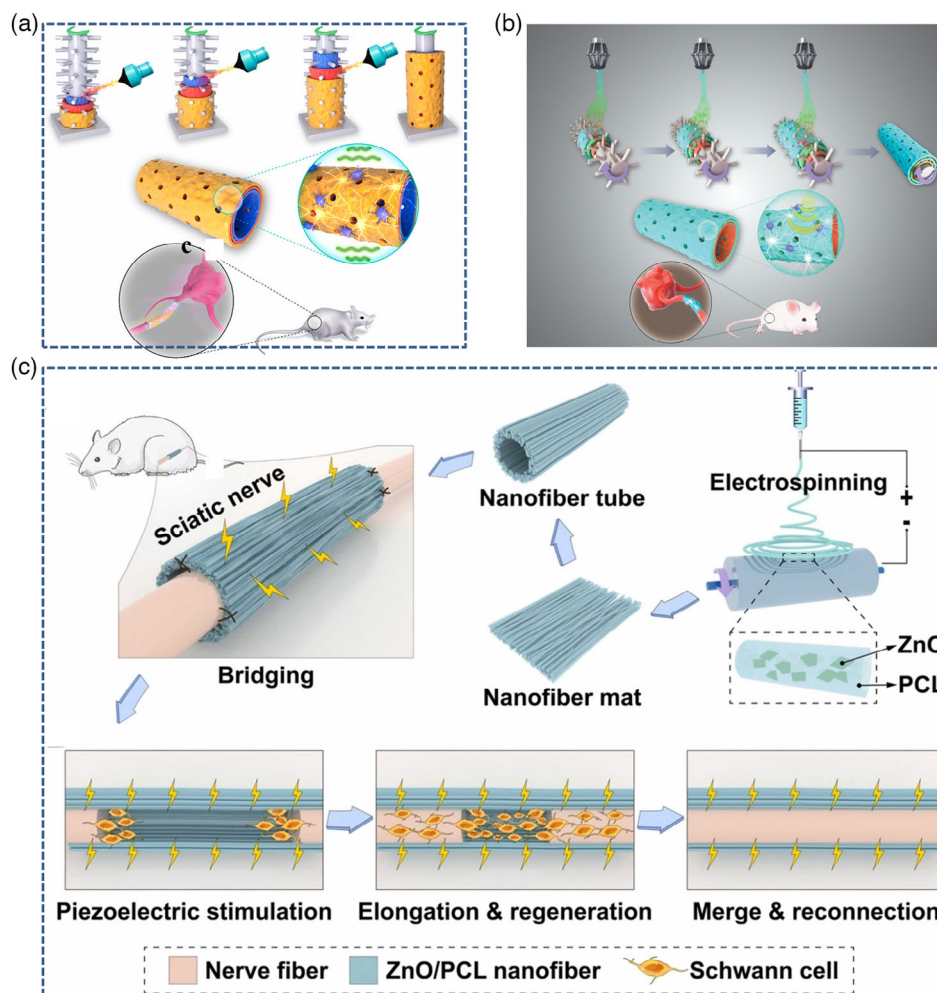


Figure 4. a) Functionalized BNNS@PCL were prepared by 3D layer-by-layer droplet spraying. b) 3D injectable multilayer biofabrication protocol for polycaprolactone (PCL) catheters containing zinc oxide (ZnO). c) Electrospinning PCL with ZnO nanofiber pads is wrapped into nanofiber tubes and then implanted into the rat sciatic nerve. PZNF provides piezoelectric stimulation for Schwann cell recruitment and regeneration of damaged axons, and eventually reconnects the axons. a) Reproduced with permission.^[79] Copyright 2021, Elsevier. b) Reproduced with permission.^[80] Copyright 2020, WILEY-VCH. c) Reproduced with permission.^[81] Copyright 2022, Elsevier.

or ROS. Therefore, dressings are commonly required to promote wound healing. Wound dressings need to meet certain prerequisites, namely, nontoxicity, tissue compatibility, biodegradability, antibacterial activity, good moisturizing properties, and sufficient physical and mechanical strength.^[82] Piezoelectric polymer NFs not only meet the above requirements for dressing materials but they can also regulate cell growth, migration, and proliferation *in vivo* through electrical stimulation.

Wang et al. comprehensively studied the effects of the electrospinning parameters on P(VDF-TrFE) NFs (Figure 5a).^[83] They implanted optimized electrospun scaffolds into rats to harvest mechanical energy and promote cell proliferation and arrangement. The implanted P(VDF-TrFE) NF scaffolds generated voltages and currents up to 6 mV and 6 nA, respectively, by slightly pulling on the rat thigh (implantation site), indicating that the mechanical force generated by the daily activities of the rat generated sufficient piezoelectric output to stimulate cellular activity. Confocal fluorescence micrographs confirmed the

perfect growth and alignment of fibroblasts along the direction of the NFs, with a 1.6-fold increase in cell proliferation.

The most popular inorganic photocatalytic nanomaterials are titanium dioxide (TiO₂) NPs, which were developed for photodynamic bacterial sterilization and have the advantage of having a lower resistance than conventional antibiotics. The high band gap, small light absorption zone, and quick electron-hole recombination of TiO₂ prevent it from being an effective photocatalyst *in vivo*. Yu et al. created TiO₂/BTO/Au multilayer coaxial heterostructured nanorod arrays by intercalating a ferroelectric semiconductor BaTiO₃ nanolayer between TiO₂ nanorods and AuNPs (Figure 5b).^[84] In the UV/visible range, the TiO₂/BTO/Au heterostructure demonstrated improved ROS formation and high incident photoelectron conversion efficiencies. They also proposed a photodynamic method, primarily based on the plasma properties of the nanorod array and piezoelectric effect, for increased ROS production. The antibacterial effectiveness of TiO₂/BTO/Au against

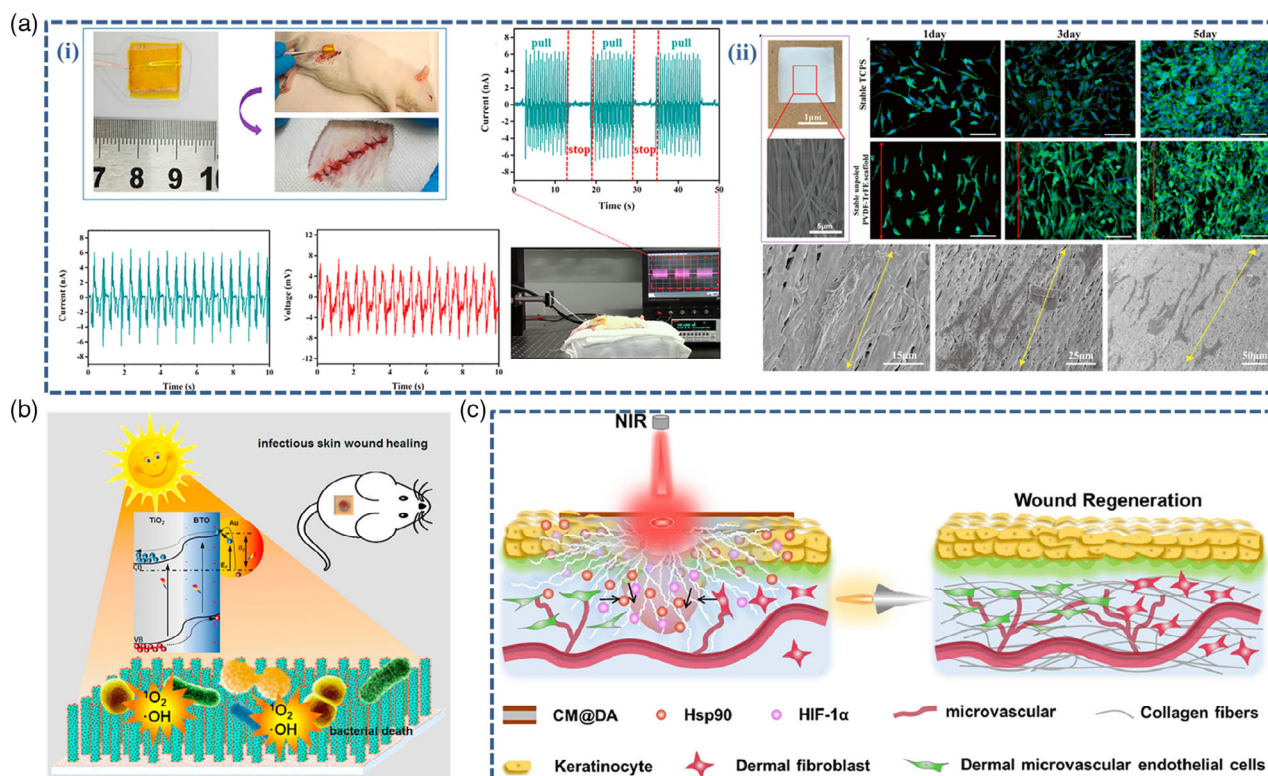


Figure 5. a-i) Image of preimplantation P (VDF-TrFE) nanofiber stent (left) and demonstration of the subcutaneous thigh area of implanted rats. The implanted P(VDF-TrFE) nanofiber scaffold produces current output and voltage output. Intermittent pulling of the mouse thigh results in the current output of the implanted stent, and the image of the experimental device. a-ii) Scanning electron microscope (SEM) and fluorescence microscopy images of invitro cytocompatibility of fibroblast cells on the P(VDF-TrFE) nanofiber scaffolds. b) Multilayer coaxial heterostructure TiO₂/BaTiO₃/Au nanorod arrays are used to enhance photodynamic performance as antimicrobial coatings. c) Schematic of chitosan film CM@DA for wound healing. a) Reproduced with permission.^[83] Copyright 2018, Elsevier. b) Reproduced with permission.^[84] Copyright 2018, Elsevier. c) Reproduced with permission.^[85] Copyright 2020, Elsevier.

Escherichia coli and *Staphylococcus aureus* as high as 99.9% under simulated sunlight irradiation, which enhanced wound regeneration in mice infected with *S. aureus*.

It has been clinically demonstrated that electrical stimulation can promote wound healing; however, the need for large equipment has limited the application of electrical stimulation. High temperatures can increase blood flow, affect enzyme activity, and activate cell signaling pathways for tissue regeneration. Chen et al. constructed a polydopamine(PBT)-coated chitosan (CM@DA) film and used it for wound healing by combining the piezoelectric effect of chitosan and the photothermal effect of PBT (Figure 5c).^[85] In vitro experiments demonstrated that the CM@DA film possessed outstanding piezoelectric and photothermal effects, which promoted the healing of full-thickness wounds in mice. Immunohistochemical staining demonstrated that CM@DA upregulated heat shock proteins and hypoxia-inducible factor (HIF-1 α) during wound healing.

3.2. Antitumor Therapy

Tumor tissues often forms pathological blood vessels that lead to local hypoxia and affect the efficiency of blood transport, hindering drug transport and therapeutic effects on tumors. Inducing

tumor vascular normalization with antiangiogenic drugs is a new strategy for treating tumors.^[86] However, antiangiogenic drugs have limitations such as side effects and strict administration procedures. Studies have shown that exogenous electrical stimulation can reduce angiogenesis at tumor sites.^[87] Sen et al. employed nutlin-3a-loaded nonfunctional polymer piezoelectric NPs that could remotely respond to ultrasound stimulation to block the angiogenic activity of human brain microvascular endothelial cells. This study opens up a new avenue for viable therapies to inhibit angiogenesis.^[87f] Marino et al. proposed a biocompatible piezoelectric NPs-based platform consisting of BTNPs functionalized with HER2 antibodies (Ab-BTNPs) capable of targeting and remotely stimulating HER2-positive breast cancer cells. This study has important guiding significance for the research of nanomaterial delivery/targeting in vivo.^[87e] These studies have important guiding significance for drug targeting and inhibiting angiogenesis behavior and provide important research methods for tumor therapy. Li et al. created tetragonal-polarized BaTiO₃ (P-BTO) piezoelectric NPs with improved the electromechanical conversion efficiency for the electrical stimulation-induced normalization of tumor blood vessels under ultrasound (Figure 6a).^[88] The results demonstrated that P-BTO NPs promoted normalization of blood vessels at the

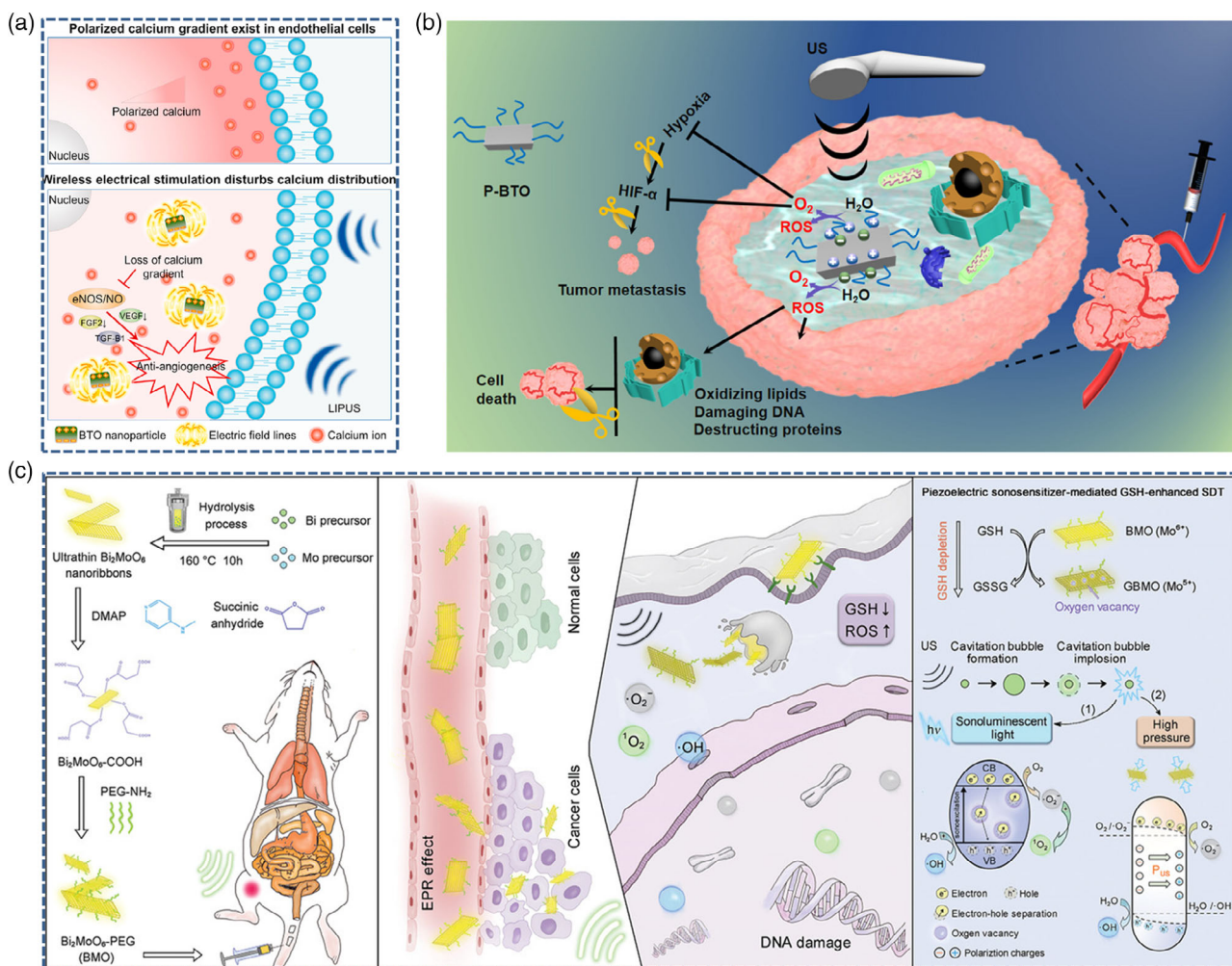


Figure 6. a) BTO nanoparticles regulate angiogenesis under LIPUS. b) Schematic diagram of tumor therapy induced by piezoelectric catalytic effects of P-BTO nanoparticles. c) Schematic diagram of a two-dimensional piezoelectric Bi₂MoO₆ acoustic sensitizer for GSH-enhanced acoustic dynamics therapy. a) Reproduced with permission.^[88] Copyright 2022, Elsevier. b) Reproduced with permission.^[89] Copyright 2021, American Chemical Society. c) Reproduced with permission.^[90] Copyright 2021, WILEY-VCH.

tumor site, thereby improving hypoxia. The combination of P-BTO and the chemotherapeutic drug DOX exhibited excellent therapeutic effects against cancer.

SDT is a commonly used method for the minimally invasive treatment of deep tumors, in which apoptosis through the generated ROS is another strategy for piezoelectric nanomaterials for antitumor therapy. Hypoxia is a typical feature of the tumor microenvironment and is associated with overexpression of HIF-1 α , which in turn is related to tumor metastasis. Since hypoxia inhibits the production of ROS in antitumor therapy, it is important to increase the oxygen concentration at the tumor site. Wang et al. fabricated ultras-small tetragonal BaTiO₃ NPs coated with DSPE-PEG2000 (P-BTO) (Figure 6b).^[89] Under ultrasonic irradiation, the surface of the P-BTO NPs generated an unbalanced charge, which triggered redox reactions that generated ROS and oxygen. A similar phenomenon was not observed for large-sized BaTiO₃ NPs and NWs. Both in vitro and in vivo experiments have demonstrated the production of large

amounts of ROS and oxygen. Lung sections from tumor-bearing mice showed reduced cancer metastasis. Therefore, piezoelectric NPs are a promising approach for treating clinically metastatic cancers that lack effective treatments.

Glutathione, as an abundant reducing substance in the tumor environment, helps tumor cells resist oxygen oxidative stress and reduces the therapeutic effect. Dong et al. fabricated a 2D piezoelectric Bi₂MoO₆ nanoribbons (BMONRs) (Figure 6c).^[90] The BMONRs could react with glutathione to generate GSH-activated BMONRs (GBMONRs) with oxygen vacancies, which hindered the recombination of electron-hole pairs and generated piezoelectric effects under cavitation, thereby improving the ROS production efficiency. GBMONRs possess a piezoelectric effect and oxygen vacancies while depleting glutathione in tumors, which is a “one stone and three birds” antitumor strategy based on ROS. Furthermore, because bismuth can significantly attenuate X-rays, BMONRs can also be used as contrast agents for tumor CT imaging to detect therapeutic effects.

3.3. Antibacterial Therapy

Infections caused by bacteria threaten the lives and health of millions of people annually. The misuse of antibiotics has caused bacteria to evolve resistance; therefore, there is an urgent need to develop new antibacterial strategies that are free of antibiotics. Because electron transport plays an important role in the energy chain of bacteria, piezoelectric materials can theoretically inhibit bacterial growth and metabolism through electrical stimulation.^[91] Moreover, piezoelectric materials can also achieve antibacterial therapy through ROS generated by SDT.

SDT is a pathogen elimination method with high spatial and temporal selectivity, and sonosensitizers with high biocompatibility and piezoelectric efficiency are key to achieving efficient treatment. Wu et al. synthesized Au@BTO nanocrystals by decorating AuNPs onto BaTiO₃ nanocubes using chemical reduction (Figure 7a).^[92] AuNPs and BaTiO₃ can form Schottky junctions, which promote the separation of electron-hole pairs at the piezoelectric ceramic/metal interface under the action of ultrasound, ultimately improving the ROS generation efficiency. *In vitro* bacterial tests showed that Au@BTO was highly effective against representative gram-negative and gram-positive bacteria, with a 99.23% *E. coli* kill rate. The Au@BTO nanocrystals further promoted wound healing by improving the migration of fibroblasts and macrophages.

Osteomyelitis treatment is difficult in orthopedics. Currently, systemic long-term antibiotic therapy combined with surgical debridement is the mainstay of recalcitrant bone infection treatments. Therefore, it is urgently necessary to find a quick, noninvasive, and antibiotic-free method for treating osteomyelitis. Feng et al. fabricated a composite structure (RBC-HNTM-MoS₂) composed of a hollow metal-organic framework (HNTM), MoS₂ nanosheets, and red cells (RBC) for the SDT of osteomyelitis (Figure 7b).^[93] MoS₂ nanosheets, as piezoelectric materials, form heterojunctions with the HNTM. The efficiency of ROS formation could be improved using ultrasonically induced piezoelectric polarization at the heterogeneous interface of HNTM-MoS₂. Simultaneously, the MoS₂ nanosheets increased the asymmetrical shape of the HNTM, resulting in a strong ultrasound-propelling ability. The resulting ROS and powerful mechanical force killed methicillin-resistant *S. aureus* within 15 minutes of ultrasound treatment with an antimicrobial efficiency of 98.5%, successfully eliminating bone infections and inhibiting bone loss and inflammation.

Polymer and ceramic composite materials are often used as synthetic bone materials; however, the piezoelectric effect of ceramic materials cannot be fully exerted owing to the large dielectric difference between polymers and ceramics. The introduction of conductive phases as micro-capacitors can improve this situation. Silver NPs (Ag NPs) can be used as ideal

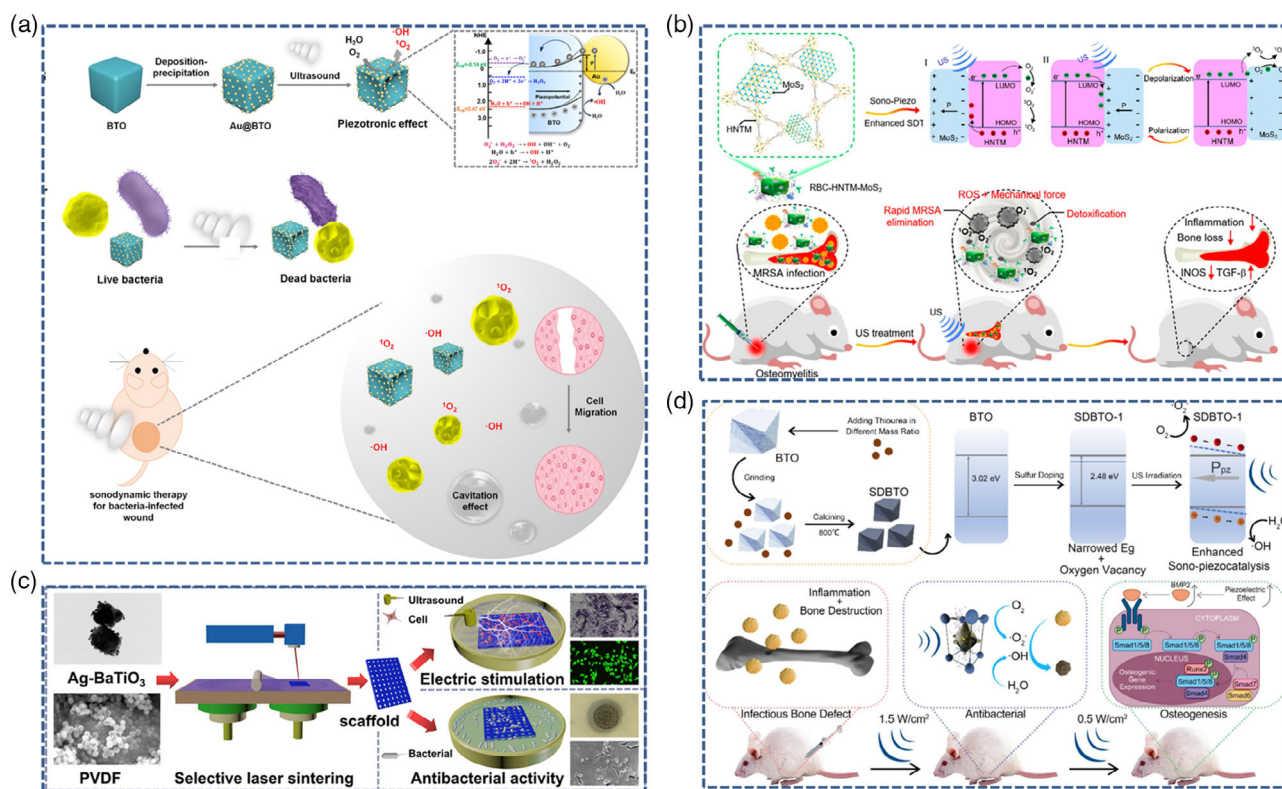


Figure 7. a) Schematic diagram of acoustic dynamic antibacterial Au@BTO piezoelectric nanocomposites. b) Osteomyelitis treating and rapid MRSA removal by acoustic catalytic mechanism of RBC-HNTM-MoS₂. c) Schematic diagram of piezoelectric and antimicrobial activity of barium titanate-reinforced polymer scaffolds of strawberry-like silver decorative, d) piezoelectric catalytic mechanism of antibacterial osteogenesis therapy of sulfur-doped barium titanate piezoelectric catalyst. a) Reproduced with permission.^[92] Copyright 2022, American Chemical Society. b) Reproduced with permission.^[93] Copyright 2020, Elsevier. c) Reproduced with permission.^[94] Copyright 2022, Elsevier. d) Reproduced with permission.^[95] Copyright 2022, Elsevier.

conductive additive phases due to their good biocompatibility and conductivity, as well as a broad spectrum of bactericidal capacity and no bacterial resistance. Shuai et al. designed a composite scaffold (PVDF/4Ag-PBT) in which AgNPs were modified on BaTiO₃ NPs coated with PBT and then doped into PVDF scaffolds (Figure 7c).^[94] The AgNPs could not only act as a conductive phase to enhance the polarized electric field strength on BaTiO₃ but also possessed ideal antimicrobial activity by releasing silver ions (Ag⁺) and generating ROS. The experimental results showed that the output current and voltage of the PVDF/4Ag-PBT holder were 50% and 40% higher than those of the PVDF/PBT holder, respectively. *In vitro* cell experiments showed that PVDF/4Ag-PBT promoted osteoblast proliferation and differentiation and exhibited good antibacterial activity against *E. coli*.

Lei et al. constructed an ultrasonically responsive sulfur-regulated BaTiO₃ nanomaterial with suitable oxygen vacancies (SDBTO-1) for the treatment of clinical refractory deep-seated bone infections (Figure 7d).^[95] The built-in electric field generated by the piezoelectric effect inhibited the recombination of electron holes, while the oxygen vacancies trapped electrons and oxygen, which promoted the generation of ROS. *In vitro* experiments demonstrated that the synthesized SDBTO-1 possessed a higher d_{33} and ROS generation efficiency than BTO-1. SDBTO-1 exhibited excellent antibacterial properties, with an antibacterial efficiency of 97.12% against *S. aureus*. Furthermore, ultrasound-activated SDBTO-1 upregulated the TGF- β signaling pathway via a moderate piezoelectric signal, thereby promoting the osteogenic differentiation of human bone marrow mesenchymal stem cells. SDBTO-1 successfully healed tibial bone defects in rats infected with *S. aureus* and achieved bone regeneration while suppressing inflammation.

3.4. Cell Force Detection

Cells generate a cell traction force (CTF) during movement, migration, contraction, relaxation, and stretching. Although these forces are extremely small, they exert profound biological effects. Together with biochemical signals, CTF coordinates and regulates life processes and plays key roles in cell proliferation, differentiation, apoptosis, tumor metastasis, wound healing, and embryonic development. It is difficult to differentiate certain malignant cells from normal cells only by morphological analysis; therefore, cellular traction measurements, as a complement, have important implications for monitoring some physiological phenomena and disease treatment. Therefore, it is very important for the study of cell biology to understand how CTF affects cell function and how much CTF is generated by cells in different states.

Owing to their piezoelectricity, silicon NWs (SiNWs) have been shown to be probes with high spatial resolution that can be used to quantify physiological processes.^[96] Using aligned SiNW arrays as nanoprobe, Li et al. devised a technique for measuring the maximal CTF in three different cell lines, namely, normal mammalian cells, benign cells (L929), and malignant cells (HeLa).^[97] Figure 8a shows a schematic illustration of SiNW arrays for quantifying cellular traction, which shows that the CTFs of the cells caused the NWs to bend inward. The results

of AFM and finite element method (FEM) calculations showed that cancer cells exhibited significantly larger CTFs than normal cells. This research methodology and its results may be useful for disease diagnosis, drug development, and tissue engineering.

In 2012, Niu et al. proposed a method based on SiNW arrays to assess the mechanical behavior of individual normal mammalian cells, benign cells (L929), and malignant cells (HeLa).^[98] The movement of cells cultured on the SiNW array caused the NWs to bend, which represents the pulling force of different cells. The elastic moduli of the prepared SiNW arrays were tested before cell culture. The relationship between the applied lateral force and related tip displacement of the SiNWs was determined using FEM simulations. This study provides a new method for cell-level diagnosis and makes a significant contribution to the study of the mechanical and migration properties of single cells.

In 2015, Peng et al. first constructed a NW array of InGaN/GaN multiple quantum wells (0.8 μm diameter, 1.2 μm height, 4 μm spacing, and 6350 dpi resolution) based on the piezoelectric optoelectronic effect.^[99] The use of this material solved the opacity problem of traditional silicon-based materials, and the InGaN/GaN multiple quantum well NW arrays could emit light at 460 nm when irradiated with 405 nm excitation light. The piezoelectric charges generated under pressure/strain successfully modulated the photoluminescence intensity of the InGaN/GaN multiple quantum wells. In 2021, Zheng et al. further improved the aspect ratio of InGaN/GaN multiple quantum well NWs and optimized the unit density of the NW array according to the size of the CTF to make it more suitable for measuring CTF (Figure 8b-i).^[100] The NW diameter, height, and array spacing of the fabricated InGaN/GaN multiple quantum wells were 150, 1500, and 800 nm, respectively, and the spatial resolution reached 31 750 dpi (Figure 8b-ii). To explore whether the NW array could dynamically realize force imaging in real time, self-contracting cardiomyocytes were used as the research object of CTF. Through the contraction and relaxation of cardiomyocytes, the CTF was applied to the piezoelectric material beneath the cells. The positive and negative piezoelectric charges generated by the optoelectronic nanoantenna array modulated the photoluminescence intensity of the quantum well. The spontaneously contracting cardiomyocytes and their underlying luminescent nanoantenna arrays were dynamically imaged using confocal laser microscopy with a temporal resolution of approximately 333 ms, and the real-time correspondence between the CTF and photoluminescence intensity changes was established. The CTF measurement range of the InGaN/GaN multiple quantum wells was 0.17–10 μN , with a detection sensitivity of 15 nN nm⁻¹, good optical stability, and repeatability (Figure 8b-iii).

3.5. Controlled Drug Release

On-demand drug delivery has attracted the attention of many researchers. As various stimuli-responsive materials have been developed, it has become possible to modulate drug release using various external or internal stimuli. Among these, electrostimulated drug delivery systems have great potential because of their ease of integration with sensors or chips and their precise temporal and spatially controlled release capabilities.

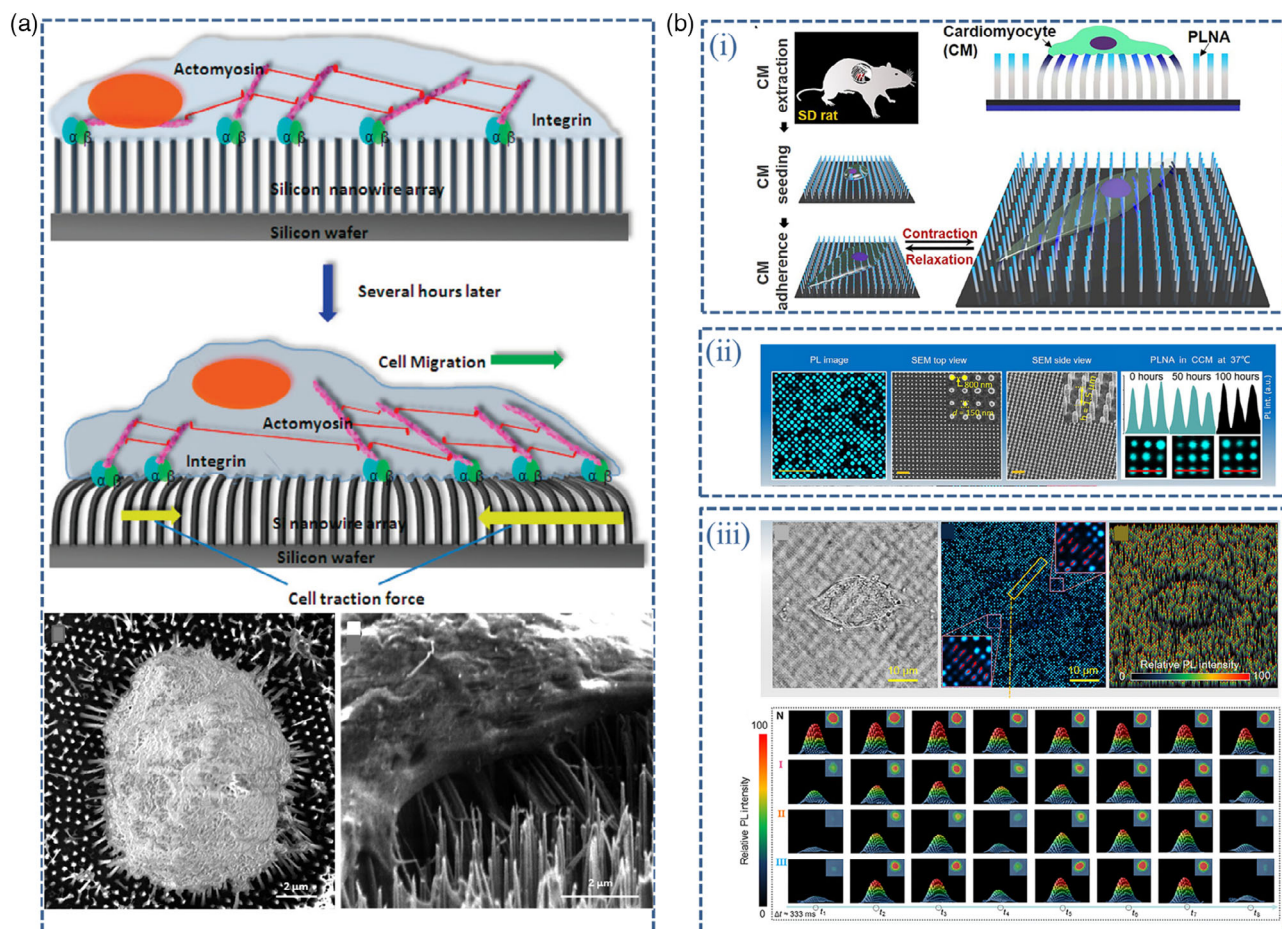


Figure 8. a) Schematic illustration of Si NW arrays for quantifying cellular traction b-i) Schematic diagram of the CTF detection process using the PLNA array. ii) Nanowire morphology of InGaN/GaN multiple quantum wells and PL stability of the PLNA array under. iii) The relationship between the cell force and the photoluminescence intensity and the time-threshold change diagram of the intensity were constructed by the NWs of InGaN/GaN multiple quantum wells. a) Reproduced with permission.^[97] Copyright 2009, American Chemical Society. b) Reproduced according to the terms of the CC-BY license.^[100]

Piezoelectric nanomaterials can remotely deliver localized voltages to cells and tissues. Owing to the direct piezoelectric effect, nanomaterials produce electrical potential on their surfaces in response to mechanical deformation, a phenomenon known as electromechanical transduction. Harmless mechanical activation, such as ultrasound, can remotely activate these materials.

In recent years, the use of various piezoelectric nanostructures for controlled drug delivery via electrical stimulation has been intensively investigated. Piezoelectric fields can be generated almost anywhere without the need for complex or time-consuming instrumentation, which is a significant advantage in emergency situations. However, this is fundamentally different from the potential generated by an electrochemical workstation. Zhang et al. proposed an active drug-releasing material that can respond to widespread mechanical disturbances in human motion.^[101] The mechanism of the release enhancement was that mechanical disturbances caused by random and alternately positive and negative piezoelectric potentials encouraged the release of tiny charged molecules. Functionalization of this material was achieved by combining a piezoelectric dielectric flexible film of

rGO-PEI/PVDF-HFP with a cross-linked LbL multilayer (PAH/PAMAM)_{10.5} (Figure 9b-ii). The number of bilayers and ionic strength affected the release enhancement efficiency. In this study, the authors applied it as an enhanced-release anti-nausea/vomiting drug on the surface of a round disposable gastric lavage tube. The ability to apply medicine more easily in emergency scenarios and the ability to maximize drug release from the matrix represent two exceptional benefits of this controlled drug release technology (Figure 9b-i).

Pucci et al. created piezoelectric hybrid lipid-polymeric NPs (PNPs) with a peptide (ApoE) to help them more easily cross the blood-brain barrier.^[102] These particles included the nongonotoxic medication, nutlin-3a. The PNPs were able to induce a cellular response in terms of Ca²⁺ channel activation in response to ultrasonic exposure, demonstrating the creation of an efficient electrical cue (Figure 9a-i). The therapeutic efficacy of the nutlin-loaded PNPs was significantly enhanced by ultrasound stimulation, despite mild cytotoxicity against T98G glioblastoma cells. In the sonicated environment, the reduced actin polymerization, invasive ability, and migratory ability of T98G cells were

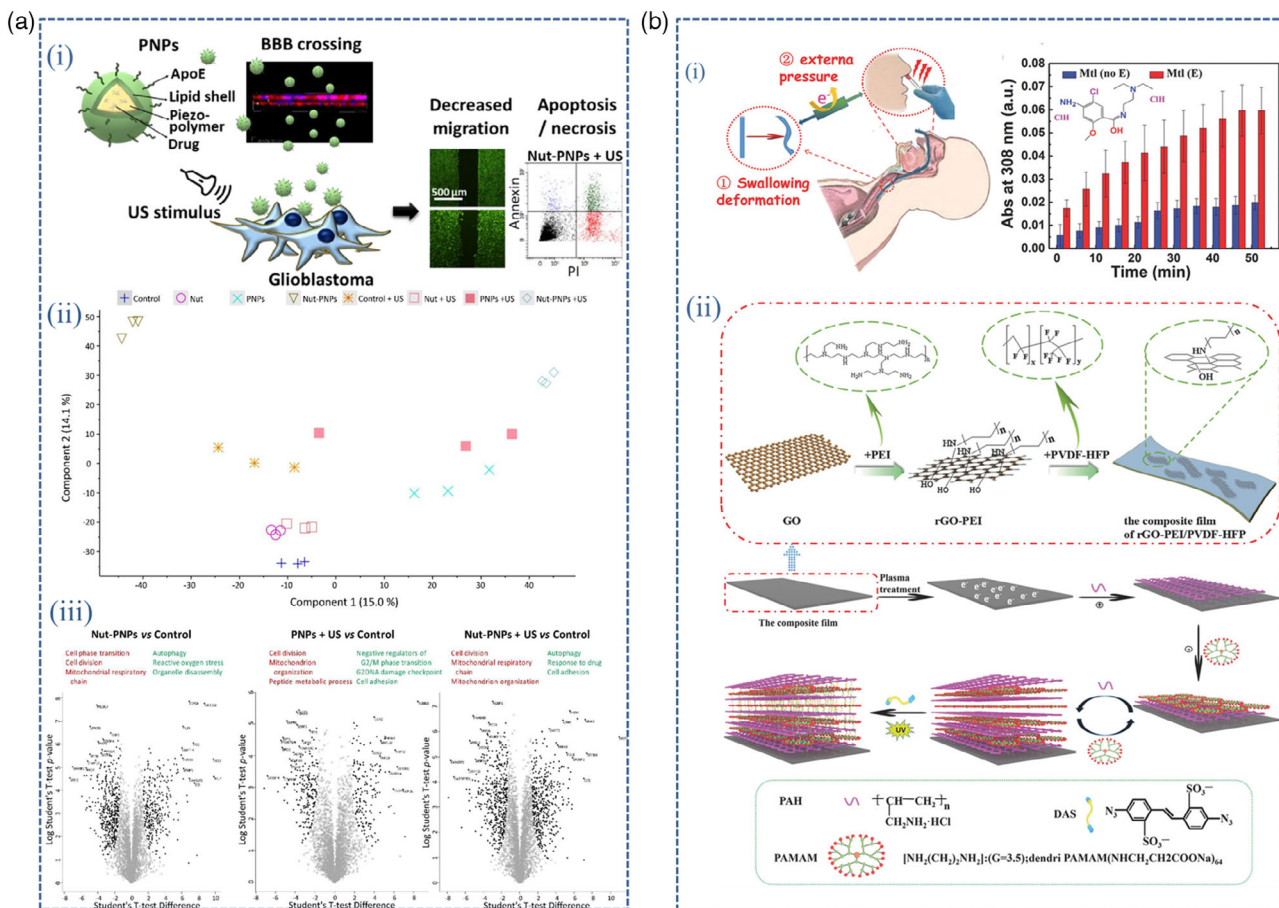


Figure 9. a-i) Schematic of ultrasound-responsive nutlin-loaded nanoparticles for combined chemotherapy and piezoelectric treatment of glioblastoma cells, ii) Proteomic analysis in T98G cells. b-i) Application diagram of disposable gastric lavage tube. ii) Schematic diagram of the fabrication process of cross-linked LbL (PAH/PAMAM)_n multilayer films on a piezoelectric-dielectric composite substrate. a) Reproduced with permission.^[102] Copyright 2022, Elsevier. b) Reproduced with permission.^[101] Copyright 2018, WILEY-VCH.

associated with nutlin-loaded PNPs. From the proteomic analysis, the important gene ontologies involved in this combination therapy are the “inhibition of cell division,” “promoting autophagy,” and “promoting cell adhesion” pathways (Figure 9a-ii). The outcomes unmistakably demonstrated the potential of ultrasonic stimulation and biocompatible organic piezoelectric NPs in the treatment of highly invasive and aggressive tumors, such as glioblastoma.

3.6. Pathological/Physiological Indicator Monitoring

The electromotive force produced when a mechanical force is applied to a piezoelectric material can be measured using piezoelectric sensors, which exploit the piezoelectric effect. They primarily measure the force by translating the received data into electrical charges and other values. They are based on the electromechanical energy-conversion principle.^[103] The development and application of biopiezoelectric nanomaterials provide the possibility for the application of piezoelectric sensors in the monitoring of physiological indicators. Feng et al. reported a core/shell PVDF/dopamine (DA) NF with a high β phase content

and self-aligned polarization properties.^[104] The authors crystallized the β phase by introducing DA as a heterogeneous nucleating agent into the PVDF electrospinning solution. The $-NH_2$ group in the DA molecule interacted with the $-CF_2$ group in PVDF and formed stable hydrogen bonds. The in situ nucleation of β -phase PVDF was made possible by the strong intermolecular interactions that occurred between the negatively charged $-CF_2$ groups and the positively charged $-NH_2$ groups in the PVDF chain as a result of hydrogen bonding and dipole interactions. To monitor diaphragm movement and arterial pulsation, PVDF/DA NFs were implanted into the diaphragm around the abdominal and femoral arteries of mice (Figure 10a). This allowed the detection of breathing patterns and arterial stiffness in various physiological situations. The results showed that the sensing response was consistent with the measured blood pressure changes, and its high sensitivity ensured real-time and accurate detection. Additionally, it successfully identified elastic changes in the peripheral artery walls, which are crucial for the early detection and medical prevention of acute and chronic cardiovascular illnesses. The device was implanted in the gastrocnemius region of mice to verify the in vivo biocompatibility and mechanical stability. When removed several weeks after implantation, histological images of the implanted

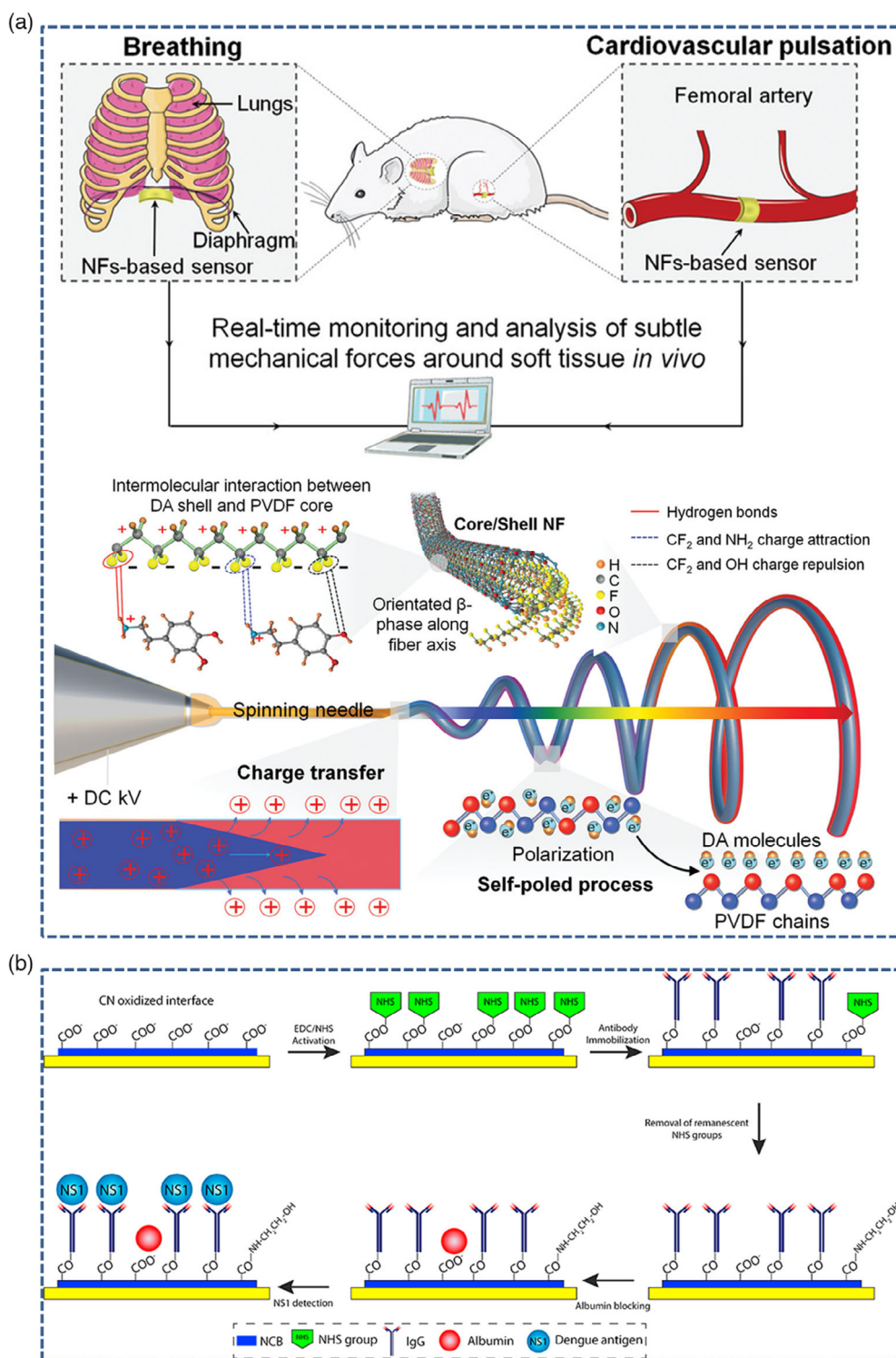


Figure 10. a) Schematic diagram of preparation and *in vivo* application of PVDF/DA core/shell NF. b) Schematic diagram of immunochip assembly. a) Reproduced with permission.^[104] Copyright 2020, Wiley-VCH. b) Reproduced with permission.^[105] Copyright 2017, Elsevier.

area showed no obvious inflammation or cytotoxicity. This indicated that the PVDF/DA NF-based sensor had excellent biocompatibility and could maintain a long-term stable sensing performance in biological environments.

Low-cost piezoelectric devices offer a wide range of clinical applications as fast diagnostic tools for various disorders. However, nonspecific antigen recognition, poor molecular probe adhesion, and sample dilution remain major disadvantages that

prevent their use in routine diagnostics. Pirich et al. used a cellulose nanocrystal (CN) film to functionalize a commercial piezoelectric sensor and attach a monoclonal antibody to the NS-1 dengue antigen (Figure 10b).^[105] Before the experiment, the piezoelectric sensor was coated with a thin layer of bacterial CNs,

which made the surface more sensitive and flexible for the attachment of monoclonal immunoglobulin G (IgGNS1) and facilitated the specific detection of dengue nonstructural protein 1 (NS1). Through the experimental comparison method, it was found that the CN surface could immobilize $2.30 \pm 0.5 \text{ mg m}^{-2}$ of IgGNS1.

Table 1. Types, principles, and applications of biopiezoelectric nanomaterials.

Piezoelectric nanomaterials	Working principle	Outcome	References
Whitlockite nanoparticles (WH NPs)	Ultrasound induces piezoelectric stimulation	Enhance osteogenesis differentiation	[25]
PVFT-BGM scaffold	Simulates the electrical environment of bones and releases osteogenesis mineral ions such as Ca^{2+} , P^{4+} .	Simulates the structure of the periosteum and promotes osteogenesis differentiation	[76]
GaN/AlGaN heterogeneous structure	Direct electrical stimulation	Promote osteogenesis differentiation	[77]
Boron nitride nanosheets (BNNS)	Ultrasound induces piezoelectric stimulation	Accelerated myelin regeneration and axonal growth in defective areas	[79]
ZnO/PCL	Mechanical stimulation is generated by a treadmill to induce piezoelectric effects	Improved recovery from severe nerve defects in rats within 18 weeks.	[80]
PZNF	Direct piezoelectric stimulation	Shortens the connection of regenerative axons (within four weeks).	[81]
(P(VDF-TrFE)) nanofibers	The mechanical force generated by daily activities produces a piezoelectric output	Promotes wound healing	[83]
TiO ₂ /BTO/Au	Piezoelectric effects and plasma effects enhance PDT	Antibacterial and wound healing	[84]
Polydopamine-coated Chitosan (CM@DA)	The piezoelectric effect is combined with the photothermal effect	Wound healing	[85]
P-BTO NPs	Electrical stimulation is produced under ultrasound conditions	Normalization of tumor vessels	[88]
Ultrasmall quadrilateral P-BTO NPs	Under ultrasound irradiation, electrical stimulation is generated, relieving hypoxia at the tumor site.	Kills tumor cells and inhibits tumor metastasis.	[89]
Bi ₂ MoO ₆ nanoribbons (BMONRs)	A piezoelectric effect is produced under ultrasound conditions, reacting with glutathione.	Contrast and inhibition of tumors	[90]
Au@BTO	A piezoelectric effect is produced under ultrasound conditions	Antibacterial and promotes wound healing	[92]
RBC-HNTM-MoS ₂	Ultrasonically induced piezoelectric effects enhance ultrasonic propulsion capability	Antibacterial and inhibits bone loss	[93]
PVDF/4Ag-PBT	Ultrasound-induced piezoelectric effect, releasing silver ions.	Exhibits good antibacterial activity against <i>Escherichia coli</i> .	[94]
SDBTO	Ultrasound activates the piezoelectric signal	Cures bacterial infections	[95]
Si NWs	By culturing cells on Si-NW arrays, the CTFs of the cells cause the NWs to bend inwards to generate electrical signals	Quantify maximum CTF in three different cell lines, namely, normal mammalian cells, benign cells (L929), and malignant cells (HeLa) methods	[96]
SiNW arrays	By culturing cells on Si NWs arrays, the maximum pulling force of different cells was measured by quantitatively analyzing the bending of the NWs.	To study the mechanical properties of single cells and their migration properties	[98]
InGaN/GaN multiple quantum wells NWs	The positive and negative piezoelectric charges generated by the cardiomyocyte movement act on the piezoelectric material to adjust the photoluminescence intensity of the quantum well.	The real-time correspondence between cell traction force and photoluminescence intensity changes was established.	[100]
rGO-PEI/PVDF-HFP with LbL multilayers of crosslinked (PAH/PAMAM) _{10,5}	The film deformations were converted into electrostatic fields which induced dielectric energy preservation inside the same film, leading to an enhanced piezoelectric potential	To facilitate either a drug application in emergent situations or to avoid wasting expensive drugs by maximizing drug release from the matrix.	[101]
Nutlin-3a-loaded ApoE-functionalized P(VDF-TrFE) NPs	Remotely activated with ultrasound-based mechanical stimulations to induce drug release and to locally deliver anticancer electric cues.	Less invasive, more focused cancer therapy, reduces the resistance of BGM to drugs	[102]
Core/shell PVDF/DA NFs	Diaphragm motion and arterial pulsation deform material to create piezoelectric effect	The PVDF/DA NFs-based sensor has good biocompatibility and can maintain long-term stable sensing performance in biological environments	[104]
CN thin films	Virus changes vibrational frequency of materials	Follow NS1 recognition	[105]

The system could detect NS1 protein in serum by only tenfold dilutions in the range of $0.01^{-10} \mu\text{g mL}^{-1}$ using QCM and QCM-D. The detection limits of the two devices were $0.1 \mu\text{g mL}^{-1}$ for QCM-D and $0.32 \mu\text{g mL}^{-1}$ for QCM. Therefore, QCM-D and QCM devices can be used to track NS1 recognition and have potential for more sensitive, rapid, and/or cheaper dengue diagnostic assays.

The application of piezoelectric nanomaterials in biomedicine is gaining increasing attention.^[106] This section summarized the applications of piezoelectric nanomaterials in tissue engineering, antitumor and antimicrobial therapy, cellular force mapping, controlled drug release, and monitoring of pathological/physiological indicators and provided specific examples. **Table 1** presents a systematic summary of the results.

4. Conclusions and Outlook

This article reviewed the fundamental principles, classifications, and applications of piezoelectric nanomaterials in tissue engineering, antitumor and antimicrobial therapy, cellular force mapping, controlled drug release, and monitoring of pathological/physiological indicators. As tunable electromechanical conversion materials, piezoelectric nanomaterials can exert various effects on biological tissues through direct electrical stimulation or free radicals generated by acoustic catalysis, thereby affecting cell proliferation, migration, differentiation, and phenotype. However, there are still some interesting problems in the biological application of piezoelectric materials that deserve further exploration. For example, although numerous studies have explored the molecular mechanisms by which piezoelectric materials affect cellular behavior through electrical stimulation or free radicals, it is still unclear that we have understood the full range of potential signaling pathways. Additionally, whether piezoelectric materials can regulate gene expression and immune responses remains to be further explored. Due to the existence of these problems that are not yet fully understood, piezoelectric materials have been limited in biological applications.

Although piezoelectric nanomaterials have become a popular research topic in the biomedical field in the past decade and have been widely used in many fields, there are still some limitations to their practical application, such as the exact mechanism of action in vivo, potential toxicity, feasibility of stimulation, and measurement of the piezoelectric output of piezoelectric materials in vivo. We hope that these issues will be addressed in future research.

Advances in piezoelectric materials will broaden our understanding of the discipline and promote the integration of different disciplines. In terms of material design, with the improvement in synthesis technology in the era of atomic engineering, it is expected that multifunctional piezoelectric composite nanomaterials with high biocompatibility will be synthesized in the future, which will further broaden their applications in biomedical engineering. Furthermore, piezoelectric biomaterials are bound to promote the development of some emerging disciplines, such as electrogenetics and bioelectronics, and their electromechanical conversion effects also provide energy solutions for the promotion of brain-computer interfaces, artificial

intelligence, and metaverse technologies. Therefore, piezoelectric nanomaterials broaden our understanding of biological systems from new perspectives, enabling more powerful life regulation and monitoring.

Acknowledgements

J.Y.J. and C.Y.Y. contributed equally to this work. This study was supported by the National Key Research and Development Program of China (2021YFB3201200), Beijing Natural Science Foundation (JQ20038, L212010), the National Natural Science Foundation of China (T2125003, 61875015, 51902344), and the Strategic Priority Research Program of Chinese Academy of Sciences (XDA16021101). The English in this document has been polished by Wiley Editing Services.

Conflict of Interest

The authors declare no conflict of interest.

Keywords

biomedical engineering applications, electrical stimulation, piezoelectric nanomaterials, reactive oxygen species, sonodynamic therapy

Received: June 23, 2022

Revised: September 16, 2022

Published online:

- [1] J. Curie, P. Curie, *Bull. Minéral.* **1880**, 3, 90.
- [2] M. Chazono, H. Watanabe, Y. Yanase, *Phys. Rev. B* **2022**, 105, 024509.
- [3] S. Horiuchi, J. Y. Tsutsumi, K. Kobayashi, R. Kumai, S. Ishibashi, *J. Mater. Chem. C* **2018**, 6, 4714.
- [4] S. M. Chang, H. Muramatsu, C. Nakamura, J. Miyake, *Mater. Sci. Eng. C* **2000**, 12, 111.
- [5] X. Lv, X.-X. Zhang, J. Wu, *J. Mater. Chem. A* **2020**, 8, 10026.
- [6] M. Smith, S. Kar-Narayan, *Int. Mater. Rev.* **2022**, 67, 65.
- [7] D. R. Schipf, G. H. Yesner, L. Sotelo, C. Brown, M. D. Guild, *Addit. Manuf.* **2022**, 55, 102804.
- [8] a) E. Fukada, *J. Phys. Soc. Jpn.* **1955**, 10, 149; b) J. Sun, H. Guo, J. Ribera, C. Wu, K. Tu, M. Binelli, G. Panzarasa, F. W. M. R. Schwarze, Z. L. Wang, I. Burgert, *ACS Nano* **2020**, 14, 14665.
- [9] a) M. H. Shamos, L. S. Lavine, *Nature* **1967**, 213, 267; b) P. Yu, C. Ning, Y. Zhang, G. Tan, Z. Lin, S. Liu, X. Wang, H. Yang, K. Li, X. Yi, Y. Zhu, C. Mao, *Theranostics* **2017**, 7, 3387.
- [10] a) R. Ding, Y. Lyu, Z. Wu, F. Guo, W. F. Io, S.-Y. Pang, Y. Zhao, J. Mao, M.-C. Wong, J. Hao, *Adv. Mater.* **2021**, 33, 2101263; b) Y. H. Yu, X. D. Wang, *Adv. Mater.* **2018**, 30, 1800154.
- [11] Y. Qin, X. Wang, Z. L. Wang, *Nature* **2008**, 451, 809.
- [12] S. Xu, Y. W. Yeh, G. Poirier, M. C. McAlpine, R. A. Register, N. Yao, *Nano Lett.* **2013**, 13, 2393.
- [13] T. Ke, H. Chen, H. Sheu, J. Yeh, H. Lin, C. Lee, H. Chiu, *J. Phys. Chem. C* **2008**, 112, 8827.
- [14] Z. W. Pan, Z. R. Dai, Z. L. Wang, *Science* **2001**, 291, 1947.
- [15] Z. Deng, Y. Dai, W. Chen, X. Pei, J. Liao, *Nanoscale Res. Lett.* **2010**, 5, 1217.
- [16] Y. Qi, N. T. Jafferis, K. Lyons Jr., C. M. Lee, H. Ahmad, M. C. McAlpine, *Nano Lett.* **2010**, 10, 524.
- [17] C. Chang, V. H. Tran, J. Wang, Y. K. Fuh, L. Lin, *Nano Lett.* **2010**, 10, 726.
- [18] J. Zhang, *Nano Energy* **2019**, 58, 568.

- [19] M. H. Zhao, Z. L. Wang, S. X. Mao, *Nano Lett.* **2004**, *4*, 587.
- [20] W. Q. Liao, D. W. Zhao, Y. Y. Tang, Y. Zhang, P. F. Li, P. P. Shi, X. G. Chen, Y. M. You, R. G. Xiong, *Science* **2019**, *363*, 1206.
- [21] a) L. F. George, E. A. Bates, *Front. Cell Dev. Biol.* **2022**, *10*, 772230; b) M. Sheth, L. Esfandiari, *Front. Oncol.* **2022**, *12*, 846917.
- [22] Y. Li, P.-S. Wang, G. Lucas, R. Li, L. Yao, *Stem Cell Res. Ther.* **2015**, *6*, 41.
- [23] a) X. Zhang, L. Li, J. Ouyang, L. Zhang, J. Xue, H. Zhang, W. J. N. T. Tao, *Nano Today* **2021**, *39*, 101196; b) J. Wang, J. Lin, L. Chen, L. Deng, W. Cui, *Adv. Mater.* **2022**, *34*, 2108325.
- [24] a) X.-F. Wang, M.-L. Li, Q.-Q. Fang, W.-Y. Zhao, D. Lou, Y.-Y. Hu, J. Chen, X.-Z. Wang, W.-Q. Tan, *Bioactive Mater.* **2021**, *6*, 230; b) M. Zhao, B. Song, J. Pu, T. Wada, B. Reid, G. Tai, F. Wang, A. Guo, P. Walczysko, Y. Gu, T. Sasaki, A. Suzuki, J. V. Forrester, H. R. Bourne, P. N. Devreotes, C. D. McCaig, J. M. Penninger, *Nature* **2006**, *442*, 457.
- [25] V. K. Kaliannagounder, N. P. M. J. Raj, A. R. Unnithan, J. Park, S. S. Park, S.-J. Kim, C. H. Park, C. S. Kim, A. R. K. Sasikala, *Nano Energy* **2021**, *85*, 105901.
- [26] H. Chen, O. Simoska, K. Lim, M. Grattieri, M. Yuan, F. Dong, Y. S. Lee, K. Beaver, S. Weliwatte, E. M. Gaffney, S. D. Minter, *Chem. Rev.* **2020**, *120*, 12903.
- [27] a) D.-M. Shin, S. W. Hong, Y.-H. Hwang, *Nanomaterials* **2020**, *10*, 123; b) M. Ge, D. Xu, Z. Chen, C. Wei, Y. Zhang, C. Yang, Y. Chen, H. Lin, J. Shi, *Nano Lett.* **2021**, *21*, 6764.
- [28] V. Jarkov, S. J. Allan, C. Bowen, H. Khanbareh, *Int. Mater. Rev.* **2021**, *67*, 683.
- [29] K. Kapat, Q. T. H. Shubhra, M. Zhou, S. Leeuwenburgh, *Adv. Funct. Mater.* **2020**, *30*, 1909045.
- [30] R. A. Surmenev, T. Orlova, R. V. Chernozem, A. A. Ivanova, A. Bartaszyte, S. Mathur, M. A. Surmeneva, *Nano Energy* **2019**, *62*, 475.
- [31] F. Ali, W. Raza, X. Li, H. Gul, K.-H. Kim, *Nano Energy* **2019**, *57*, 879.
- [32] M. A. Fernandez-Yague, A. Trotier, S. Demir, S. A. Abbah, A. Larranaga, A. Thirumaran, A. Stapleton, S. A. M. Tofail, M. Palma, M. Kilcoyne, A. Pandit, M. J. Biggs, *Adv. Mater.* **2021**, *33*, 2008788.
- [33] E. Fukada, Y. Ando, *J. Polym. Sci. A* **1972**, *10*, 565.
- [34] a) A. Stapleton, M. R. Noor, J. Sweeney, V. Casey, A. L. Kholkin, C. Silien, A. A. Gandhi, T. Soulimane, S. A. M. Tofail, *Appl. Phys. Lett.* **2017**, *111*, 142902; b) H. Athenstaedt, *Ann. NY Acad. Sci.* **1974**, *238*, 68.
- [35] B. Yin, Y. Qiu, H. Zhang, J. Lei, Y. Chang, J. Ji, Y. Luo, Y. Zhao, L. Hu, *Nano Energy* **2015**, *14*, 95.
- [36] a) B. Jaffe, R. S. Roth, S. Marzullo, *J. Appl. Phys.* **1954**, *25*, 809; b) B. Jaffe, R. S. Roth, S. Marzullo, *J. Res. Natl. Bur. Standards* **1955**, *55*, 239.
- [37] E. Ringgaard, T. Wurlitzer, *J. Eur. Ceram. Soc.* **2005**, *25*, 2701.
- [38] F. Yan, H. Bai, Y. Shi, G. Ge, X. Zhou, J. Lin, B. Shen, J. Zhai, *Chem. Eng. J.* **2021**, *425*, 130669.
- [39] Z. Tan, J. Xi, J. Xing, B. Wu, Q. Zhang, Q. Chen, J. Zhu, *J. Eur. Ceram. Soc.* **2022**, *42*, 3865.
- [40] Z. Xiong, B. Tang, X. Zhang, C. Yang, S. Zhang, *Ceram. Int.* **2018**, *44*, 19058.
- [41] a) S. Rezvani, Y. S. Chuo, J. Lee, S. S. Park, *Ceram. Int.* **2022**, *48*, 14684; b) Z. Li, Y. Cho, X. Li, X. Li, A. Aimi, Y. Inaguma, J. A. Alonso, M. T. Fernandez-Diaz, J. Yan, M. C. Downer, G. Henkelman, J. B. Goodenough, J. Zhou, *J. Am. Chem. Soc.* **2018**, *140*, 2214; c) X. Tian, G. L. Brennecke, X. Tan, *Adv. Funct. Mater.* **2020**, *30*, 2004607.
- [42] H.-S. Wu, B. T. Murti, J. Singh, P.-K. Yang, M.-L. Tsai, *Adv. Sci.* **2022**, *9*, 2104703.
- [43] a) H. P. Maruska, J. J. Tietjen, *Appl. Phys. Lett.* **1969**, *15*, 327; b) R. Dingle, K. L. Shaklee, R. F. Leheny, R. B. Zetterstrom, *Appl. Phys. Lett.* **1971**, *19*, 5.
- [44] H. Amano, N. Sawaki, I. Akasaki, Y. Toyoda, *Appl. Phys. Lett.* **1986**, *48*, 353.
- [45] a) D. M. Bagnall, Y. F. Chen, Z. Zhu, T. Yao, S. Koyama, M. Y. Shen, T. Goto, *Appl. Phys. Lett.* **1997**, *70*, 2230; b) S. Chu, G. Wang, W. Zhou, Y. Lin, L. Chernyak, J. Zhao, J. Kong, L. Li, J. Ren, J. Liu, *Nat. Nanotechnol.* **2011**, *6*, 506.
- [46] R. Araneo, G. Lovat, P. Burghignoli, C. Falconi, *Adv. Mater.* **2012**, *24*, 4719.
- [47] Z. L. Wang, J. H. Song, *Science* **2006**, *312*, 242.
- [48] A. Cafarelli, A. Marino, L. Vannozzi, J. Puigmartí-Luis, S. Pané, G. Ciofani, L. J. A. N. Ricotti, *ACS Nano* **2021**, *15*, 11066.
- [49] Z. L. Wang, W. Wu, C. Falconi, *MRS Bull.* **2018**, *43*, 922.
- [50] L. Lu, W. Ding, J. Liu, B. Yang, *Nano Energy* **2020**, *78*, 105251.
- [51] A. Datta, Y. S. Choi, E. Chalmers, C. Ou, S. Kar-Narayan, *Adv. Funct. Mater.* **2017**, *27*, 1604262.
- [52] Z. Pi, J. Zhang, C. Wen, Z.-B. Zhang, D. Wu, *Nano Energy* **2014**, *7*, 33.
- [53] B. Mohammadi, A. A. Yousefi, S. M. Bellah, *Polym. Test.* **2007**, *26*, 42.
- [54] a) V. Sencadas, R. Gregorio Jr., S. Lanceros-Mendez, *J. Macromol. Sci. B-Phys.* **2009**, *48*, 514; b) S. Mishra, L. Unnikrishnan, S. K. Nayak, S. Mohanty, *Macromol. Mater. Eng.* **2019**, *304*, 1800463.
- [55] Z. Liu, S. Li, J. Zhu, L. Mi, G. Zheng, *ACS Appl. Mater. Interfaces* **2022**, *14*, 11854.
- [56] K. Eom, S. Na, J.-K. Kim, H. Ko, J. Jin, S. J. Kang, *Nano Energy* **2021**, *88*, 106244.
- [57] X. Yuan, X. Gao, X. Shen, J. Yang, Z. Li, S. Dong, *Nano Energy* **2021**, *85*, 105985.
- [58] K. S. Ramadan, D. Sameoto, S. Evoy, *Smart Mater. Struct.* **2014**, *23*, 033001.
- [59] C. Miao, L. Reid, Y. W. Hamad, *Appl. Mater. Today* **2021**, *24*, 101082.
- [60] S. Bera, S. Guerin, H. Yuan, J. O'Donnell, N. P. Reynolds, O. Maraba, W. Ji, L. J. W. Shimon, P.-A. Cazade, S. A. M. Tofail, D. Thompson, R. Yang, E. Gazit, *Nat. Commun.* **2021**, *12*, 2634.
- [61] F. Yang, J. Li, Y. Long, Z. Zhang, L. Wang, J. Sui, Y. Dong, Y. Wang, R. Taylor, D. Ni, W. Cai, P. Wang, T. Hacker, X. Wang, *Science* **2021**, *373*, 337.
- [62] Z. Zhang, S. Liu, Q. Pan, Y. Hong, Y. Shan, Z. Peng, X. Xu, B. Liu, Y. Chai, Z. Yang, *Adv. Mater.* **2022**, *34*, 2200864.
- [63] R. Liu, G. Hu, M. Dan, Y. Zhang, L. Li, Y. Zhang, *Nano Energy* **2020**, *72*, 104678.
- [64] W. Wu, L. Wang, Y. Li, F. Zhang, L. Lin, S. Niu, D. Chenet, X. Zhang, Y. Hao, T. F. Heinz, J. Hone, Z. L. Wang, *Nature* **2014**, *514*, 470.
- [65] Z. Liu, L. Xu, Q. Zheng, Y. Kang, B. Shi, D. Jiang, H. Li, X. Qu, Y. Fan, Z. L. Wang, Z. Li, *ACS Nano* **2020**, *14*, 8074.
- [66] X. Qian, Y. Zheng, Y. Chen, *Adv. Mater.* **2016**, *28*, 8097.
- [67] G. Maddirala, T. Searle, X. Wang, G. Alici, V. Sencadas, *Appl. Mater. Today* **2022**, *26*, 101361.
- [68] B. Tandon, J. J. Blaker, S. H. J. A. B. Cartmell, *Acta Biomater.* **2018**, *73*, 1.
- [69] A. Cafarelli, A. Verbeni, A. Poliziani, P. Dario, A. Menciasci, L. Ricotti, *Acta Biomater.* **2017**, *49*, 368.
- [70] a) C. F. Guimarães, L. Gasperini, A. P. Marques, R. L. Reis, *Nat. Rev. Mater.* **2020**, *5*, 351; b) S. R. Shin, Y.-C. Li, H. L. Jang, P. Khoshkhalagh, M. Akbari, A. Nasajpour, Y. S. Zhang, A. Tamayol, A. Khademhosseini, *Adv. Drug Deliv. Rev.* **2016**, *105*, 255; c) M. Rahmati, D. K. Mills, A. M. Urbanska, M. R. Saeb, J. R. Venugopal, S. Ramakrishna, M. Mozafari, *Progr. Mater. Sci.* **2021**, *117*, 100721.
- [71] M. Montorsi, G. G. Genchi, D. De Pasquale, G. De Simoni, E. Sinibaldi, G. Ciofani, *Biotechnol. Bioeng.* **2022**, *119*, 1965.
- [72] G. G. Genchi, E. Sinibaldi, L. Ceseracciu, M. Labardi, A. Marino, S. Marras, G. De Simoni, V. Mattoli, G. Ciofani, *Nanomed. Nanotechnol. Biol. Med.* **2018**, *14*, 2421.
- [73] a) N. Kimelman-Bleich, G. Pelled, Y. Zilberman, I. Kallai, O. Mizrahi, W. Tawackoli, Z. Gazit, D. Gazit, *Mol. Ther.* **2011**, *19*, 53; b) T. Geach, *Nat. Rev. Endocrinol.* **2016**, *12*, 248.

- [74] W. Liu, X. Li, Y. Jiao, C. Wu, S. Guo, X. Xiao, X. Wei, J. Wu, P. Gao, N. Wang, Y. Lu, Z. Tang, Q. Zhao, J. Zhang, Y. Tang, L. Shi, Z. Guo, *ACS Appl. Mater. Interfaces* **2020**, *12*, 51885.
- [75] C. Wu, Y. Tang, B. Mao, K. Zhao, S. Cao, Z. Wu, *Surf. Coat. Technol.* **2021**, *405*, 126510.
- [76] F. Zhao, C. Zhang, J. Liu, L. Liu, X. Cao, X. Chen, B. Lei, L. Shao, *Chem. Eng. J.* **2020**, *402*, 126203.
- [77] C. Zhang, W. Wang, X. Hao, Y. Peng, Y. Zheng, J. Liu, Y. Kang, F. Zhao, Z. Luo, J. Guo, B. Xu, L. Shao, G. Li, *Adv. Funct. Mater.* **2021**, *31*, 2007487.
- [78] a) C. R. Carvalho, J. Silva-Correia, J. M. Oliveira, R. L. Reis, *Adv. Drug Deliv. Rev.* **2019**, *148*, 308; b) G. Otto, *Nat. Rev. Neurosci.* **2021**, *22*, 456; c) A. Marino, G. G. Genchi, V. Mattoli, G. Ciofani, *Nano Today* **2017**, *14*, 9; d) Y. Shan, X. Cui, X. Chen, Z. Li, *WIREs Nanomed. Nanobiotechnol.* **2022**, e01827.
- [79] Y. Qian, Y. Xu, Z. Yan, Y. Jin, X. Chen, W.-E. Yuan, C. J. N. E. Fan, *Nano Energy* **2021**, *83*, 105779.
- [80] Y. Qian, Y. Cheng, J. Song, Y. Xu, W.-E. Yuan, C. Fan, X. Zheng, *Small* **2020**, *16*, 2000796.
- [81] R. Mao, B. Yu, J. Cui, Z. Wang, X. Huang, H. Yu, K. Lin, S. G. F. Shen, *Nano Energy* **2022**, *98*, 107322.
- [82] G. S. Schultz, R. G. Sibbald, V. Falanga, E. A. Ayello, C. Dowsett, K. Harding, M. Romanelli, M. C. Stacey, L. Teot, W. Vanscheidt, *Wound Repair Regen.* **2003**, *11*, S1.
- [83] A. Wang, Z. Liu, M. Hu, C. Wang, X. Zhang, B. Shi, Y. Fan, Y. Cui, Z. Li, K. Ren, *Nano Energy* **2018**, *43*, 63.
- [84] X. Yu, S. Wang, X. Zhang, A. Qi, X. Qiao, Z. Liu, M. Wu, L. Li, Z. L. J. N. E. Wang, *Nano Energy* **2018**, *46*, 29.
- [85] Y. Chen, M. Ye, L. Song, J. Zhang, Y. Yang, S. Luo, M. Lin, Q. Zhang, S. Li, Y. J. A. M. T. Zhou, *Appl. Mater. Today* **2020**, *20*, 100756.
- [86] A. Marino, E. Almici, S. Migliorin, C. Tapeinos, M. Battaglini, V. Cappello, M. Marchetti, G. de Vito, R. Cicchi, F. S. Pavone, G. Ciofani, *J. Colloid Interface Sci.* **2019**, *538*, 449.
- [87] a) Y. Hou, Y. Liu, C. Tang, Y. Tan, X. Zheng, Y. Deng, N. He, S. Li, *Chem. Eng. J.* **2022**, *435*, 134145; b) X. Wang, X. Zhong, L. Cheng, *Coord. Chem. Rev.* **2021**, *430*, 213662; c) N. Gong, N. C. Sheppard, M. M. Billingsley, C. H. June, M. J. Mitchell, *Nat. Nanotechnol.* **2021**, *16*, 25; d) E. Alphandéry, *J. Nanobiotechnol.* **2022**, *20*, 139; e) A. Marino, M. Battaglini, D. De Pasquale, A. Degl'Innocenti, G. Ciofani, *Sci. Rep.* **2018**, *8*, 6257; f) O. Sen, A. Marino, C. Pucci, G. Ciofani, *Mater. Today Bio.* **2022**, *13*, 100196.
- [88] C. Li, C. Xiao, L. Zhan, Z. Zhang, J. Xing, J. Zhai, Z. Zhou, G. Tan, J. Piao, Y. J. B. M. Zhou, *Bioactive Mater.* **2022**, *18*, 399.
- [89] P. Wang, Q. Tang, L. Zhang, M. Xu, L. Sun, S. Sun, J. Zhang, S. Wang, X. J. A. N. Liang, *ACS Nano* **2021**, *15*, 11326.
- [90] Y. Dong, S. Dong, B. Liu, C. Yu, J. Liu, D. Yang, P. Yang, J. Lin, *Adv. Mater.* **2021**, *33*, 2106838.
- [91] Y. Wang, Y. Yang, Y. Shi, H. Song, C. Yu, *Adv. Mater.* **2020**, *32*, 1904106.
- [92] M. Wu, Z. Zhang, Z. Liu, J. Zhang, Y. Zhang, Y. Ding, T. Huang, D. Xiang, Z. Wang, Y. J. N. T. Dai, *Nano Today* **2021**, *37*, 101104.
- [93] X. Feng, L. Ma, J. Lei, Q. Ouyang, Y. Zeng, Y. Luo, X. Zhang, Y. Song, G. Li, L. Tan, X. Liu, C. Yang, *ACS Nano* **2022**, *16*, 2546.
- [94] C. Shuai, G. Liu, Y. Yang, F. Qi, S. Peng, W. Yang, C. He, G. Wang, G. J. N. E. Qian, *Nano Energy* **2020**, *74*, 104825.
- [95] J. Lei, C. Wang, X. Feng, L. Ma, X. Liu, Y. Luo, L. Tan, S. Wu, C. Yang, *Chem. Eng. J.* **2022**, *435*, 134624.
- [96] R. He, P. Yang, *Nat. Nanotechnol.* **2006**, *1*, 42.
- [97] Z. Li, J. Song, G. Mantini, M.-Y. Lu, H. Fang, C. Falconi, L.-J. Chen, Z. L. Wang, *Nano Lett.* **2009**, *9*, 3575.
- [98] Y. Niu, A. Qin, W. Song, M. Wang, X. Gu, Y. Zhang, M. Yu, X. Zhao, M. Dai, L. Yan, Z. Li, Y. Fan, *J. Nanomater.* **2012**, *2012*, 384671.
- [99] M. Peng, Z. Li, C. Liu, Q. Zheng, X. Shi, M. Song, Y. Zhang, S. Du, J. Zhai, Z. L. Wang, *ACS Nano* **2015**, *9*, 3143.
- [100] Q. Zheng, M. Peng, Z. Liu, S. Li, R. Han, H. Ouyang, Y. Fan, C. Pan, W. Hu, J. Zhai, Z. Li, Z. L. Wang, *Sci. Adv.* **2021**, *7*, eabe7738.
- [101] Y. Zhang, Q. An, W. Tong, H. Li, Z. Ma, Y. Zhou, T. Huang, Y. Zhang, *Small* **2018**, *14*, 1802136.
- [102] C. Pucci, A. Marino, O. Sen, D. D. Pasquale, M. Bartolucci, N. Iturrioz-Rodriguez, N. D. Leo, G. D. Vito, D. Debellis, A. Petretto, G. Ciofani, *Acta Biomater.* **2022**, *139*, 218.
- [103] N. Liu, R. Wang, S. Gao, R. Zhang, F. Fan, Y. Ma, X. Luo, D. Ding, W. Wu, *Adv. Mater.* **2021**, *33*, 2105697.
- [104] T. Li, M. Qu, C. Carlos, L. Gu, F. Jin, T. Yuan, X. Wu, J. Xiao, T. Wang, W. Dong, X. Wang, Z.-Q. Feng, *Adv. Mater.* **2021**, *33*, 2006093.
- [105] C. L. Pirich, R. A. de Freitas, R. M. Torresi, G. F. Picheth, M. R. Sierakowski, *Biosens. Bioelectron.* **2017**, *92*, 47.
- [106] a) A. Roy, D. Dwari, M. K. Ram, P. Datta, in *Food, Medical, and Environmental Applications of Nanomaterials*, Elsevier, USA, **2022**, pp. 355–377; b) A. Marino, G. G. Genchi, E. Sinibaldi, G. Ciofani, *ACS Appl. Mater. Interfaces* **2017**, *9*, 17663.



Jianying Ji received her bachelor degree at Qufu Normal University in 2017 and Master degree at Guilin University of technology in 2020. She is currently a Ph.D. candidate in Guangxi University and a joint student in Professor Li Zhou's group at Beijing Institute of Nanoenergy and Nanosystems, CAS. Her research focuses on the design and fabrication of piezoelectric nanomaterials.



Chunyu Yang received her B.E. degree in polymer material and engineering at the Hubei University in 2020. She is currently a graduate student in the China University of Petroleum (Beijing). Her work now focuses on the design of nanomaterials for photodynamics therapy.



Yizhu Shan received her bachelor's degree from the School of Pharmacy, Harbin Medical University. She is currently pursuing the Ph.D. degree at Beijing Institute of Nanoenergy and Nanosystems, Chinese Academy of Sciences. Her research interests include developing novel therapy for nervous system injury and self-powered biomedical systems.



Mingjun Sun obtained a bachelor's degree in chemical engineering technology from Shandong University of Technology in 2019. She graduated from China University of Petroleum (Beijing) majoring in chemical engineering in June 2022. She currently works in the Emergency Rescue Command and Support Center of Wudi County Emergency Management Bureau, Shandong Province.



Xi Cui received her bachelor's degree from Jilin University in the Department of Life and Sciences, Jilin, China, in 2019. Now she is a Ph.D. candidate in Beijing Institute of Nanoenergy and Nanosystems, Chinese Academy of Sciences. Her current research mainly focuses on nanogenerators and in vivo self-powered biosensors.



Lingling Xu received her bachelor and master's degrees from Sichuan University in 2015 and 2018, respectively, and her Ph.D. degree from University of Chinese Academy of Sciences in 2021. She is now a postdoctoral research fellow at the National Center for Nanoscience and Technology of China. Her research interests include the stimulus-responsive drug delivery system and biomedical systems.



Shiyuan Liang is now a Ph.D. candidate at Beijing Institute of Nanoenergy and Nanosystems, Chinese Academy of Sciences. She received her B.Sc. degree in chemical engineering at the China University of Petroleum (Beijing) in 2021. Her work now focuses on the synthesis of nanomaterials and its application in the fields of biology and energy.



Tong Li received her bachelor's degree from Bioengineering, China University of Mining and Technology in 2019 and received her master's degree at Guangxi University in 2022. Her research focuses on transcatheter flexible intracardiac pressure sensor enables interventional device for in situ blood pressure measurement.



Yijie Fan is now a Ph.D. candidate at Beijing Institute of Nanoenergy and Nanosystems, Chinese Academy of Sciences. He received his master's degree in chemical engineering at the China University of Petroleum (Beijing) in 2022. His current work focuses on the synthesis of 2D materials and their applications in biological and energy catalysis.



Dan Luo received his B.Sc. and Ph.D. degrees at Peking University Health Science Center in 2008 and 2013, respectively. He worked at Institute of Chemistry, Chinese Academy of Sciences in 2013, then transferred to China University of Petroleum-Beijing in 2015. Since 2021, he has joined the Beijing Institute of Nanoenergy and Nanosystems, Chinese Academy of Sciences as a professor. His research focuses on physiotherapy strategies based on self-powered devices.



Zhou Li received his Ph.D. from Peking University in Department of Biomedical Engineering in 2010 and bachelor's degree from Wuhan University in 2004. He joined School of Biological Science and Medical Engineering of Beihang University in 2010 as an Associate Professor. Currently, he is a Professor in Beijing Institute of Nanoenergy and Nanosystems, Chinese Academy of Sciences. His research interests include nanogenerators, in vivo energy harvesters, self-powered medical devices, and biosensors.